Modeling of River-flow Routing Using a Muskingum-and-Manning method and Application in Basin of Seine

Yan ZHAO

Directrice de recherche : Agnès Ducharne

UMR Sisyphe (UPMC)

September 27, 2006

UNIVERSITE
PIERRE & MARIE CURIE
LA SCIENCE A PARIS

ECOLE DES MINES
DE PARIS

ENGREF

Abstract

Modeling of river flow routing has been widely used to compute the water level, discharge, and storage etc. by simulating the waterflow behavior. In actual research, there are mainly two kinds of ways: hydraulic and hydrological routing approaches. Among the latter, one of the most popular is the Muskingum method.

However the general Muskingum method can only calculate the flow in a uniform river reach, which is regarded as a uniform linear reservoir. If the parameters and the inflow are known, the outflow at the outlet of the reach is easily obtained, but it does not depend on river stage, which is not deduced from the storage in the reach.

As we know, the characteristics of the stream reach have some influence on flow routing. One famous equation which connects the reaches' characteristics and flow velocity is Manning equation. Therefore in this study, we combine the Muskingum method and Manning equation to develop the so-called Muskingum-and-Manning method, which describes the variations in river stage and its influence on flow velocity and outlflow.

By testing the Muskingum and Muskingum-and-Manning methods in a simple reach and in a hypothetic regular river network, we showed the importance of the numerical integration method to achieve valid results. We showed the superiority of the 4th order Runge-Kutta method on the Euler method, and that a time step of 6hours at most was advisable. In these conditions, the simulations with both routing methods rightly reflect the influence of their different parameter, of hydrological conditions, and of the characteristics of the river bed for the Muskingum-and-Manning method. This physically-based method, combined to the numerically efficient 4th order Runge-Kutta integration method, will be the basis on full routing model, to be validated in the future, in particular in the Seine river basin.

Keywords :

Method, Muskingum, Manning, flow, simulation, application, influence, reach, characteristic

Acknowledgements

I would like to thank here all the people who contributed more or less to this work. First of all, I am grateful to my tutor, researcher at CNRS: Agnès DUCHARNE, who offered me this opportunity to programming the river flow using a hydrological routing approach in the basin and also enlightened me to find many means of study. I am so glad to have this experience which both enhance my program ability and enlarge my hydrological knowledge in practice. I feel endlessly interested in this study.

I also owe special thanks to Aurélien BARO, GIS engineer at CNRS and Simon GASCOIN, PhD student at the Pierre Marie Curie University. Aurélien BARO was my mentor in studying the software of GIS and helped me to settle these problems with patience. Simon GASCOIN was always happy to help me when I had programming problems and he gave me many good advices in my work.

Finally, I would like to thank my family who conferred me so many encouragements and hopes. This drove me to face even the most difficult conditions and gave me a lot of confidence.

Contents

List of notations

SYMBOL	UNIT	DEFINITION	CHAPTER, PARAGRAPH

Capital letters

SYMBOL	UNIT	DEFINITION	CHAPTER, PARAGRAPH
A	m²	wetted cross sectional area	§2.1
I	m³/s	inflow (upstream)	§2.1
L	m	reach length	§2.3
P	m	wetted perimeter	§3.2.1
Q	m³/s	outflow discharge	§2.1
Q_w	m³/s	weighted discharge	§4.5
R	m	hydraulic radius	§3.2.1
S	m³	storage in the reach	§2.1
T	m	reach width	§2.3
T_{lag}	s	lag time	§2.2
T_s	s	travel time	§2.3.2
V	m/s	flow velocity (instantaneous)	§2.1
Z	m	water surface elevation or stage	§2.2

Small letters

SYMBOL	UNIT	DEFINITION	CHAPTER, PARAGRAPH
k	s	wave travel time (Muskingum parameter)	§2.3
n	s/m$^{1/3}$	Manning's coefficient of roughness	§3.2.1
q	m³/s	lateral inflow or outflow	§2.1
s_0	- -	slope of riverbed	§3.2.1
t	s	time	§2.1
v_c	m/s	mean flow velocity in a reach	§3.1
x_a	m	distance along the longitudinal axis of the watercourse	§2.1
x	- -	weighting factor (Muskingum parameter)	§2.3
y	m	water depth in reach	§2.2

1. Introduction

Land surface models (LSMs) simulate the coupled water and energy fluxes from terrestrial surfaces. They are an important element of general circulation models, which are used in particular to produce scenarios of anthropogenic climate change. They can also be used in a stand-alone mode to simulate the response of runoff to various climate or land use scenarios. As for all models, validation is a mandatory step to gain confidence in the simulated projections. An interesting validation exercise for LSMs is to compare their runoff to riverflow, which integrates the runoff from the whole area upstream from the gauging station, and which is a widely available data, recorded with an interesting precision, and in many areas for several decades at least. However, runoff and riverflow are not directly comparable. Runoff is a flow per unit surface (expressed for instance in mm/d) and riverflow is the integration of the latter over the contributing area, with complex delays, related to the length and roughness of the many different water pathways from the points of runoff production to the gauging station. This transformation is often called runoff routing, and can be separated in two processes, namely the routing of runoff to the closest river reach, and the routing inside the river network, which includes the delays imposed to riverflow along the reaches, and the accumulation of riverflow at each confluence.

In this thesis, we address the question of river flow routing only. To this end, there are a lot of methods described in traditional hydrological literature that are used. These methods can be generally classified into two categories:

> (1) Hydraulic or distributed routing methods – Use both continuity and momentum equations to describe unsteady, non-uniform flow in a flow system. It is based on Saint-Venant equations, a continuity equation which describe the balance between input, storage and output in a section of river, and a momentum equation which relates the change in momentum to the applied forces (e.g., Liggett, 1975; Bathurst, 1988; Becker and Serban, 1990).

> (2) Hydrological routing methods – Use continuity equation, along with an analytical or an assumed relationship between storage and discharge within a system, in the calculation. It is also based on the continuity equation but empirical relationships are used to replace the momentum equation (e.g., Sherman, 1932; Carter and Godfrey, 1960; Cunge, 1969; Dooge et al, 1982; Wilson 1990) such as the Muskingum, Muskingum-Cunge and the Unit Hydrograph methods. A comprehensive review of hydrological flood routing methods is presented by Weinmann and Laurenson [1979]. In practice, because Saint-Venant equations are far too complex for normal requirements and require data that are difficult to obtain, hydrological routing models are used more often. [Arora et al, 2000]

The above-mentioned functions are widely accepted as hydrological routing techniques and are extensively used in engineering practice. In this study, we developed a routing procedure which has two components – the Muskingum method and Manning equation. One important goal was to simulate the variations of river stage in the reach, to better describe the dynamics of river discharge by accounting for the increase of river velocity with water stage, but also as it opens the possibility to simulate flooding above a critical stage.

In this procedure, the proportionality coefficient of Muskingum, k, which is defined no longer to be a constant parameter as usual, is variable with the change of the storage in the reach. Owing to the varying coefficient k, the result of the Muskingum method should draw closer to the running situation in reality.

This so-called Muskingum and Manning method is applied in the computational procedure with the fourth-order Runge-Kutta (RK4) numerical method to advance the flow routing through the whole integration time. By studying the sensitivities to different values of the parameters and comparing the results in different forcing cases, this method was found suitable for the general rivers.

The next chapter presents the basic equations in most flow routing methods. It starts with the mass conservation equation, and then it introduces the hydraulic and hydrological routing methods, with some examples.

We chose to work with a hydrological method (different from distributed along the reach), and we selected the widely used Muskingum method, which is detailed in chapter 3. The limitation of this method with respect to the objective of this work is that it neither describes the evolution of river stage, nor the influence of the latter on river discharge. To this end, we combined it to the Manning equation in what we called the Muskingum-and-Manning method.

Chapter 4 explains the numerical method we used to integrate both the Muskingum and the Muskingum-and-Manning schemes over time in a given reach. We showed the interest of a fourth-order Runge-Kutta method and the importance of the integration timestep to achieve a correct precision. In particular, we showed that the concern of negative outflow reported with the Muskingum method is a numerical problem which can be totally overcome with an adequate timestep.

After these theoretical considerations, Chapter 5 details the application of both the Muskingum and Muskingum-and-Manning methods to a single reach and shows, as a theoretical validation exercise, that the sensitivity of the simulated hydrologic variable to the input parameters agrees with the theory, under different hydrological forcing. This validation is generalized in a theoretical river network.

Eventually, Chapter 6 describes how the Muskingum-and-Manning method could be applied in the Seine River basin, using the runoff simulated by the Catchment-based LSM [Koster et al, 2000, Ducharne et al, 2000] as well as the morphology of the main river. This simulation work is left to be continued in the future, because we lacked for the runoff simulation results.

2 River flow routing method

In Handbook of Hydrology [Maidment, 1993, Sec. 10.1], flow routing is defined as a mathematical procedure for predicting the changing magnitude, speed, and shape of a flood wave as a function of time at one or more points along a watercourse (waterway or channel). Generally, flow routing can be classified as either lumped or distributed. All of these flow routing methods are based on the basic equation of one-dimensional flow, the mass conservation.

2.1 Fundamental equation - mass conservation

The conservation of mass along a river reach, also called continuity equation, is the fundamental principle in practice to express the water balance within a closed scope, and is defined below:

$$\frac{\partial(AV)}{\partial x_a} + \frac{\partial A}{\partial t} - q = 0 \tag{2-1}$$

V is the flow velocity in m/s; A is wetted cross section area in m²; x_a is the distance along the longitudinal axis of the watercourse; t is time interval in s; and q is lateral inflow or outflow in m³/s, which is ignored in our study.

In this differential equation (Eq. (2-1)), x_a and t are respectively the spatial and temporal dimensions of the river flow variables, A, V, and p, which can be expressed as follows:

$$A = f(x_a, t), \qquad V = f(x_a, t), \qquad p = f(x_a, t) \tag{2-2}$$

Basically, the dynamic equation is a differential equation of x_a and t (Eq. (2-1)). In hydrological methods, or lumped methods, it is replaced by a simpler relationship, which does not depend on x_a. Therefore, the flow is computed as a function of time only at one location along the watercourse, usually one reach. Hence the principle of mass conservation requires the difference between the two flows to be equal to the time rate of change of the storage S within the reach, the conservation equation can be simplified as:

$$\frac{dS(t)}{dt} = I(t) - Q(t) - q(t) \tag{2-3}$$

Where S(t) is storage in the reach, in m³; I(t) is the inflow discharge, in m³/s; Q(t) is the outflow discharge, in m³/s, which is showed in Fig. 2-1. Eq. (2-3) is often referred to as the hydrologic storage equation.
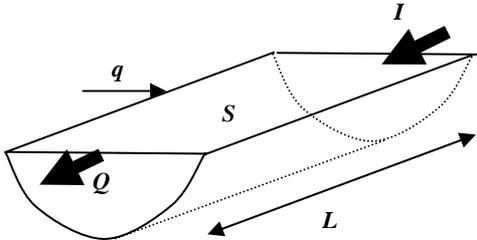

Figure 2-1. Schema of river reach

This relationship between the storage in the reach and discharge can easily define the outflow discharge Q(t) if we know the initial conditions of storage S(t=0) and the inflow I(t) at each time step, as presented in Fig. 2-2. The hatched part in this figure is the change in storage during a certain period of time (here is 1 day), and it is also the integral of the difference between inflow and outflow during this period.

In such a lumped formulation of the routing problem, the state-space vector is reduced to a single variable S(t) giving the storage in the reach at any particular instant. Eq. (2-3), when rearranged to give the outflow Q(t) as a function of the state S(t) and the input I(t), gives us the output-state equation in standard form and the insertion of this expression for the output Q(t) in Eq. (2-1) gives us the state transition equation in standard form [Dooge et al, 1982].
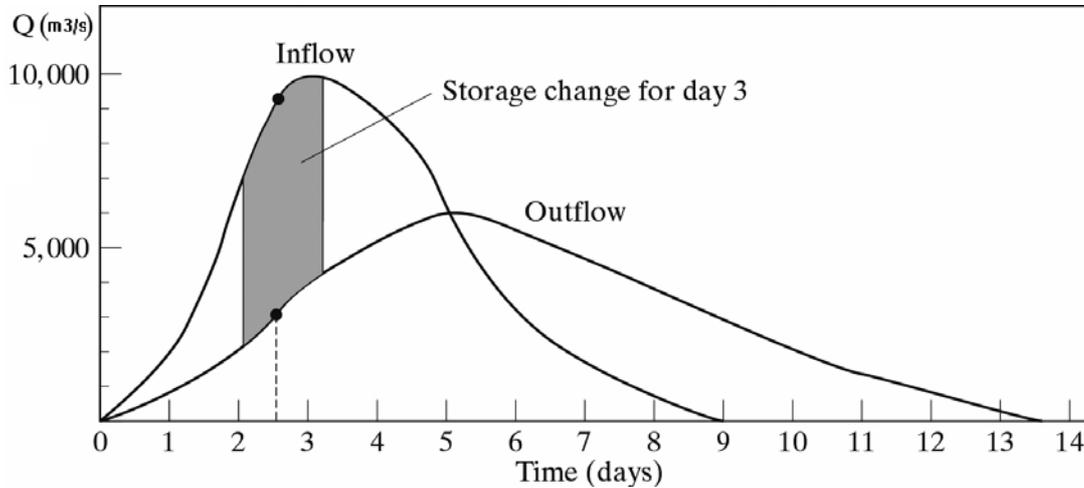

Figure 2-2. Schematic of upstream and downstream flow hydrographs

2.2 Distributed routing method

In distributed routing or hydraulic flow routing methods, the flow is computed as a function of time simultaneously at several cross sections along the watercourse and water depth (elevation) varies in space (at cross sections along the channel) as shown in Fig. 2-3.
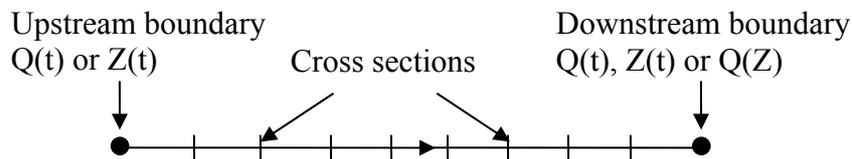

Figure 2-3. Schematic showing distributed flow routing system, where Q is discharge or flow rate and Z is water surface elevation or stage

Distributed flow routing based on the complete Saint-Venant equation is known as dynamic routing. Also, simplified form of the Saint-Venant equations, referred to as kinematic and diffusion (zero-inertia) equations, can be used for distributed flow routing.

Distributed flow routing methods can compute both the flow rate and water-surface elevation, which is useful for determining floodplain depths or required heights of structures. And it can also be used for such applications as real-time forecasting of river floods, etc.

In this study, the variations of the flow rate, velocity, and depth (elevation) in space are not required at a fine resolution, so we chose lumped routing methods which compute the flow as function of time.

4

2.3 Lumped routing method

A simplified description of unsteady flow along a watercourse (routing reach) as shown in Fig. 2-4, depicts it as a lumped process, in which the inflow I at the upstream end and the outflow Q at the end of the watercourse are functions of time.

I(t) Inflow Point   Q(t) Outflow Point

Figure 2-4. Schematic showing lumped flow routing system

Lumped flow routing methods for rivers offer the advantage of simplicity where there is an absence of significant backwater effects, and it could be applied where the depth-discharge relation is essentially single-valued, and the product of the time of rise of the hydrograph and the channel bottom slope is not small. Some common lumped models are listed in Tab. 2-1.

Table 2-1. Examples of hydrological models

Condition	Model name	Equation
$Q \neq f(S)$ and $V \neq f(S)$	Simple delay [Bolgov et al, 2002]	$Q = I(t + T_{lag})$
	Lag-and-route [Linsley, et al., 1949]	$Q = f(I(t), T_{lag})$
$Q = f(S)$ and $V \neq f(S)$	Linear reservoir [Hannah et al, 2001]	$Q = S / \tau \Leftrightarrow S = \tau . Q; \tau = L/\overline{V}$
	Muskingum [McCarthy, 1939]	$S = k \cdot [x \cdot I + (1-x)Q]; k = L/\overline{V}$
$Q = f(S)$ and $V = f(S)$	Muskingum-and-Manning [Dooge, 1982]	$k = \dfrac{n \cdot L}{\sqrt{s_o}} \left(\dfrac{L \cdot T^2 + 2 \cdot S}{T \cdot S} \right)^{2/3}$

Here, Q is outflow discharge, m^3/s, S is storage in reach, m^3, V is velocity, m/s, I is inflow discharge, m^3/s, t is time, s, T_{lag} is lag time, τ is linear coefficient, k, x are Muskingum parameters, n is manning's coefficient, $s/m^{1/3}$, s_o is riverbed slope, L is reach length, m, T is reach width, m.

2.3.1 Muskingum method

The Muskingum method, which was first proposed by McCarthy [1939], is still a subject of research [Hjelmfelt, 1985; Perumal, 1992; Gill, 1992] in the domain of flow routing calculation and some hydrological reasoning. The recent developments made it possible to link the Muskingum model, which used to be treated as an empirical concept, with hydrodynamics. Cunge [1969], who demonstrated that Muskingum method could be considered as being numerically related to the Saint-Venant equation via the diffusion wave, compared different schemes of the Muskingum method and of the convective diffusion analogy; Dooge [1973] compared the impulse responses of the Muskingum model and of the most complete linear hydrodynamic model (i.e. the linearized de Saint-Venant model) using the moment matching technique. Strupczewski & Kundzewicz [1980], Dooge et al. [1982] and Napiorkowski et al. [1981] derived the Muskingum method by lumping and linearizing distributed nonlinear models of hydrodynamics. [Kundzewicz et al, 1982]

By now, the Muskingum method is one of the most popular lumped flow routing technique used in hydrograph models, and is also employed in some cases for channel routing elements.

Dooge et al. [1982] applied this method with the hydraulic parameters of the open channel reach to various shapes of cross-section. The Manning friction, the riverbed slope, water depth, and the Froude number, were used to express the Muskingum parameters, k and x, to be variable in the simulation. It is concluded that the result is credible. Arora [1999] also introduced a flow routing scheme, which used the Manning equation for river channel flow, and the Muskingum method for routing surface runoff from upstream to downstream.

Therefore, the Muskingum method can be used to simulate river flow with variable parameters. We chose the Muskingum method in our study and introduce it in details in Sec. 3.1 (Page 8-9).

2.3.2 Lag-and-route method

Like the Muskingum method, another well-known example of handy tools for flow routing is the lag-and-route [Linsley, et al., 1949] method. It is particularly attractive for its simplicity, stability, and relative efficiency. This method initially used a linear reservoir. However, Bentura and Michel [1997] showed that using nonlinear reservoirs was significantly more efficient. They compared lag-and-route methods with linear and nonlinear routing stores and assessed these models against synthetic data obtained using the complete Saint-Venant equations solved by the Preissmann numerical scheme. Their results suggested that the higher the exponent of the routing store, the more accurately the method reproduces the routing performed by the Saint-Venant equations. Bentura and Michel [1997] provide further details on their approach and the specificities of the linear and the quadratic variants. More recently, the quadratic lag-and route model served as a basis of the routing module for the QUASAR model [Sincock and Lees, 2002]. Michel, et al. [1997] presented a new lag-and-route method where the routing reservoir is bi-quadratic. They compared this approach to the classical Hayami method.

The normal lag-and-route method comprises a relationship equation between storage and discharge as well as the conservation of mass with the travel time parameter T_s, which ensure the "routing" part of the method through a reservoir designed to dampen the hydrograph:

$$\begin{cases} \dfrac{dS(t)}{dt} = I(t) - Q(t) \\ Q(t) = \left[\dfrac{S(t)}{T_s} \right]^{\alpha} \end{cases}$$

Where T_s is the travel time parameter and has units of time; α is the exponent dimension.

Here the time step Δt is split into multi sub-intervals dt. In order to obtain an analytical solution, it is necessary to consider this time interval dt small enough so as the inflow I(t) can be considered as approximately constant I within dt. After running the routing component of the method, the outflow over the time interval is generalized with the following:

$$Q(t + dt) = \left[\frac{Q(t)^{1-\frac{1}{\alpha}} + (\alpha - 1) \cdot \dfrac{I^{2\left(1-\frac{1}{\alpha}\right)} \cdot dt}{T_s}}{1 + (\alpha - 1) \cdot \dfrac{Q(t)^{1-\frac{1}{\alpha}} \cdot dt}{T_s}} \right]^{\frac{\alpha}{\alpha - 1}} \qquad (2-4)$$

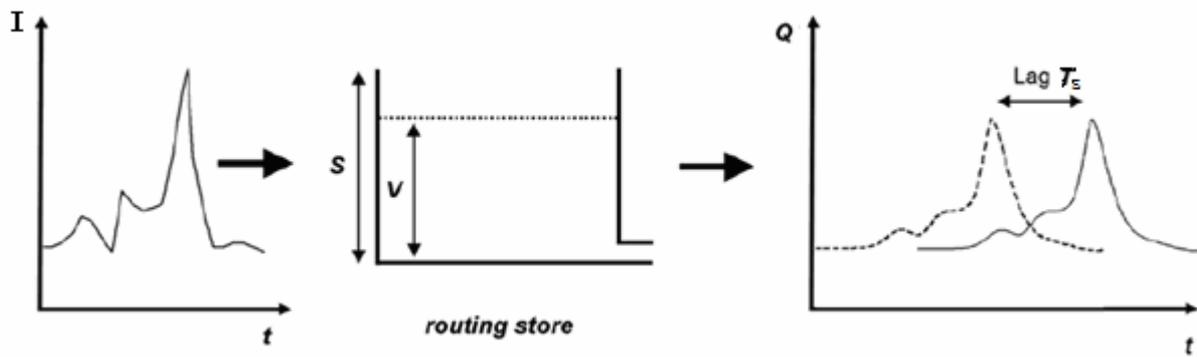This relationship between inflow and outflow can be showed in Fig. 2-5.

Figure 2-5. Schematic representation of the lag-and-route method [Michel et al, 2006]

Compared to the Muskingum method, the lag-and-route method has some disadvantages with respect to our goals for flow routing.

♦ The outflow Q(t) depends on the storage S(t) and a travel time T_s, but does not depends on the storage in the reach S(t). As in the Muskingum method, the parameters are constant.

♦ The lag time T_s should be known and constant. In practice, it is difficult to estimate the exact value of T_s.

♦ The most important thing is that in this method, we can not apply Manning equation to express the variations of velocity and outflow with the storage in the reach.

Therefore the lag-and-route method is not fit to be used as reference in this study. The simpler Muskingum is chosen to be used in following, together with the Muskingum-and-Manning method, which is derived from the Muskingum method.

3. Hydrologic routing schemes used in this study

Flow routing is a major problem in hydrological engineering. For this purpose, the so-called hydrological methods are still widely used, especially where data concerning the geometry of the channel are not available, but the volumes entering and leaving the section is known. These methods have the same structure, and are based on the conservation of mass and the relationship between storage volume, inflow as well as outflow in the river section. One of these methods and perhaps the most frequently used in practice is the Muskingum method.

3.1 Muskingum method

If the simple relationship between storage S(t) and outflow Q(t) which is presented in Eq. (2-3) is developed by adding a storage delay time k and a term involving the time derivative of the outflow Q(t), then a conceptual model is obtained consisting of two linear reservoirs in series. However if the choice of two parameters is made by assuming that the storage S(t) is linear function of the inflow I(t) as well as of the outflow Q(t), then we get the following Muskingum equation:

$$S(t) = k [x I(t)+(1-x) Q(t)] \qquad (3\text{-}1)$$

Where x is a weighting factor having the range $0 \leq x \leq 0.5$ (most streams have x values between 0.1 and 0.3) [Maidment, 1993, Sec. 10.2.3]. Thus, if the water storage in the channel is only controlled by the downstream condition, x = 0. On the contrary, x = 0.5 gives a similar weight to the inflow and outflow. It means storage is a function of average flow rate. The parameter k is the proportionality coefficient of Muskingum equation. It can be estimated as follows:

$$k = \frac{L}{v_c} \qquad (3\text{-}2)$$

Where k is the wave travel time in the reach, in s; L is the reach length in Fig. 2-1, in m; v_c is a mean velocity, constant in m/s.

From Eq. (3-1), the outflow discharge Q(t) can be calculated from the river storage S(t) and the inflow flux I(t):

$$Q(t) = \frac{S(t) - k \cdot x \cdot I(t)}{k(1-x)} \qquad (3\text{-}3)$$

This Muskingum equation represents the relationship between reach storage and discharge as a flow wave, defined by the inflow, propagates through the reach. It is used in the Muskingum method with the conservation equation, Eq. (2-3).

This method can represent the hysteresis in the relationship between reach storage and discharge, which is illustrated in Fig. 3-1. This concept is also depicted in Fig. 3-2 where the first case represents the storage in the reach during the rising limb of a hydrograph, the second case represents uniform flow, and the third case represents the storage during the falling limb of the hydrograph. This hysteresis effect is due to the different flow wave speeds during the rising and falling limb of the hydrograph. For the same river stage, the flow wave moves

faster during the rising limb of the hydrograph. The effect from this variable reach storage-discharge relationship is mimicked by the Muskingum equation as Eq. (3-1) for reach storage. [Boroughs et al, 2002].
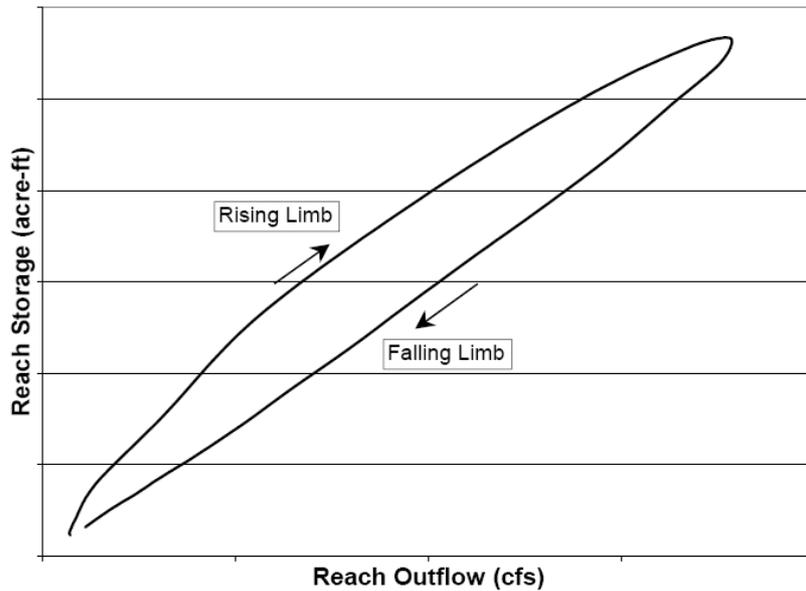

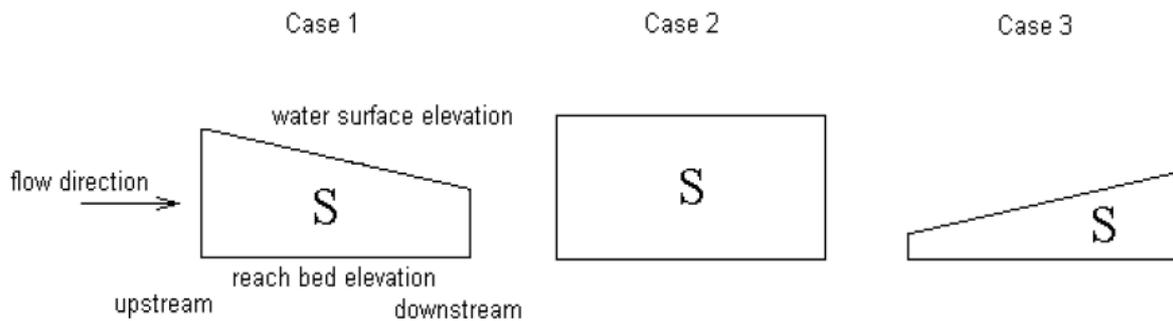Figure 3-1. Storage in a River Reach versus Reach Outflow [Boroughs et al, 2002]

Figure 3-2. Depiction of Reach Storage as a Flow Wave Propagates Downstream [Boroughs et al, 2002]

Generally speaking, the Muskingum method comprises the mass conservation and the Muskingum equation:

$$\begin{cases} \dfrac{dS(t)}{dt} = \text{I}(t) - \text{Q}(t) \\ \text{S (t)} = \text{k [x I(t)+(1-x) Q(t)]} \end{cases}$$

The Muskingum method serves to calculate the flow in a given section, with a given time increment and parameters k and x calibrated using previously measured runoff inflow and outflow (where k is the storage parameter and x is the weight factor). k and x can also be prescribed a priori, by transferring parameters validated in similar reaches.

This method enables the routing of a given discharge hydrograph downstream of a uniform river or channel reach to any desired location, and also computes the corresponding stage hydrograph as in the case of the solutions of the Saint-Venant equations. The Muskingum method, however, defines a lumped storage hydrograph for the studied reach.

3.2 Muskingum-and-Manning method

3.2.1 Manning equation

In practice, the river velocity largely depends on the parameters of environmental conditions such as the river bed condition and the river storage. The Manning - Strickler formula, one of the best known and most often used equations to calculate river flow velocity whatever the geometry of the reach, is considered to meet these demands. It is formed of common geometrical parameters as below:

$$v = \frac{1}{n} \cdot R^{2/3} \cdot s_O^{1/2}$$

(3-4)

Where v is cross-sectional average velocity, in m/s; n is the Manning coefficient of roughness, in $s/m^{1/3}$; R is the hydraulic radius, in m (illustrated in Fig. 3-3); s_o is the river slope, without dimension.

Given that Q = A·V, where A is the wetted section area of flow, Eq. (3-5) can be developed to calculate the discharge by knowing the river stage and geometry, which control A and R:

$$Q = \frac{A}{n} \cdot R^{2/3} \cdot s_O^{1/2}$$

(3-5)

The hydraulic radius R of a specific river cross section is temporally variable due to river stage dynamics. It depends on the shape of the river bed profile and the actual water level:

$$R = \frac{A}{P}$$

(3-6)

Where A is the wetted cross sectional area of flow varying as the storage in reach, in m^2; P is wetted perimeter, in m. Fig. 3-3 expresses the general wetted section area A and wetted perimeter P as well as the hydraulic radius R when the cross section is irregular.
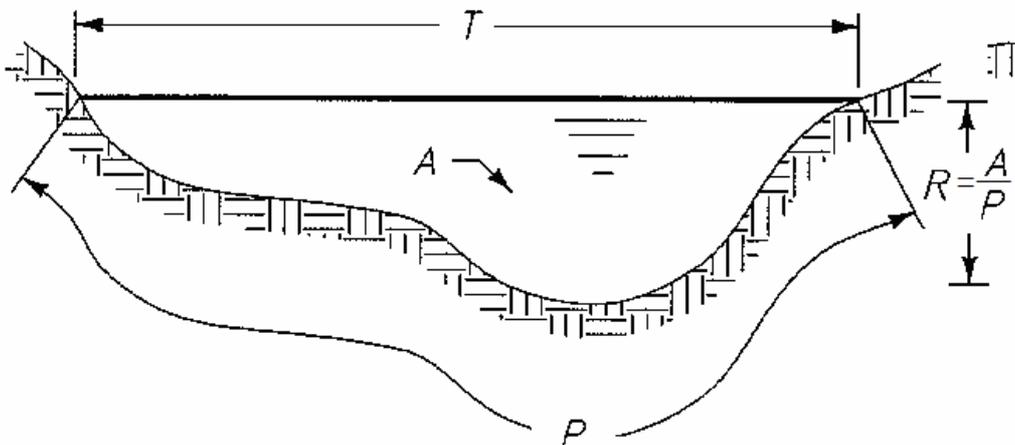
Figure 3-3. Schematic of the hydraulic radius R in an irregular flow cross section, where T is the width of water surface, in m [1]

The river slope s_0 is calculated as elevation difference between the upstream and downstream altitudes of the river bed, divided by their horizontal distance.

The Manning coefficient of roughness, n, is an empirically derived coefficient, which is dependent on many factors, including river-bottom roughness and sinuosity. Often the best method is to use photographs of river channels. Values of n typically range between 0.02 for smooth and straight rivers, to 0.075 for sinuous rivers and creeks with excess debris on the

---

[1] Water measurement manual, revised reprint 2001, http://www.usbr.gov/pmts/hydraulics_lab/pubs/wmm/chap02_11.html

river bottom or river banks [Goodwill; Fette]. From the mathematics, it follows that a greater n-value will result in a smaller value for flow velocity, thus in slower flow and smaller outflow. In Tab.3-1, here are some typical n values.

Table 3-1. Manning's n range in different type of channel [Goodwill; Fette]

Channel type	Surface material and form	Manning's Roughness Coefficient - n
River	earth, straight	0.02-0.025
	earth, meandering	0.03-0.05
	gravel (75-150mm), straight	0.03-0.04
	gravel (75-150mm), winding	0.04-0.08
	winding natural streams with weeds	0.035
	natural streams with little vegetation	0.025
Mountain streams	rocky beds	0.04-0.05
Unlined cannel	earth, straight	0.018-0.025
	rock, straight	0.025-0.045
Lined cannel	concrete	0.012-0.017
Lab. models	mortar	0.011-0.013
	perspex	0.009

3.2.2 Muskingum method with Manning equation

River flow velocity is crucial to simulate discharge hydrographs and the residence time of water in the hydrological system.

In the Muskingum method, the weighting factor x is set to be constant; k is also constant and can be related to the reach length L and a constant celerity v_c. However the flow velocities in many natural rivers are influenced by the physical channel factors and changing frequently. Here the Manning equation is introduced to describe this variable flow velocity.

We assume that the river cross section is shaped as a rectangle (Fig. 3-4), so the hydraulic radius R can be calculated as a function of river depth y and width T, which is constant:
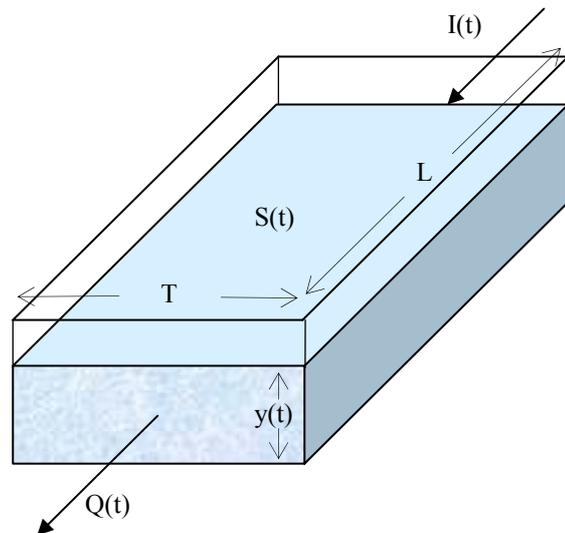
Fig.3-4 Scheme of rectangular river cross section

$$R(t) = \frac{T \cdot y(t)}{T + 2 \cdot y(t)} \qquad (3-7)$$

Where T is the reach width, in m; y is water depth or river stage in the reach, in m; t is time in seconds.

The storage in the reach is calculated as follow:

$$S(t) = L \cdot T \cdot y(t) \qquad (3-8)$$

Then y(t) is adjusted to the left side of the equal mark:

$$y(t) = \frac{S(t)}{T \cdot L} \qquad (3-9)$$

This expression is substituted in the Eq. (3-7), giving the hydraulic radius equation:

$$R(t) = \frac{T \cdot S(t)}{L \cdot T^2 + 2 \cdot S(t)} \tag{3-10}$$

With the variable hydraulic radius R(t), the average velocity v in the reach calculated by Manning equation as Eq. (3-4) is obtained as below:

$$v(t) = \frac{1}{n} \cdot R(t)^{2/3} \cdot s_O^{1/2} \tag{3-11}$$

Combining with the variable mean velocity in Eq. (3-11), the Muskingum coefficient k in Eq. (3-2) can be related to variable river channel's coefficient R(t):

$$k(t) = \frac{L \cdot n}{R(t)^{2/3} \cdot s_o^{1/2}} \tag{3-12}$$

Knowing that the hydraulic radius R(t) depends on the reach storage S(t) in Eq. (3-10), k(t) is transformed to be related to S(t):

$$k(t) = \frac{L \cdot n}{s_o^{1/2}} \cdot \left[\frac{L \cdot T^2 + 2 \cdot S(t)}{T \cdot S(t)} \right]^{2/3} \tag{3-13}$$

From the Eq. (3-13), we can get the conclusion that k(t) varies with the storage in reach during each time step. In other words, k(t) is a function of S(t), so the Eq. (3-14) can be written as follows:

$$k(S) = \frac{L \cdot n}{s_o^{1/2}} \cdot \left[\frac{L \cdot T^2 + 2 \cdot S}{T \cdot S} \right]^{2/3} \tag{3-14}$$

Substituting Eq. (3-14) into the Maskingum Eq. (3-3), we get the relationship between outflow Q and the variable storage S. So if we know the inflow I* between the timestep t_0 and t_1, and the initial storage S_0 at t_0, Q* can be calculated between t_0 and t_1 according to this equation:

$$Q^* = \frac{S_0 - k(S_0) \cdot x \cdot I^*}{k(S_0)(1-x)} \tag{3-15}$$

Eqs. (3-14) and (3-15) indicate the connection of the coefficient k and outflow Q that both depend on the variable reach storage over time. As a result, the relations are represented as k=f(S) and Q=f(S), which is the core of this method.

The combination of Eq. (3-14), (3-15) and the conservation equation (2-3) defines the Muskingum-and-Manning (simply called M-M) method, which can be used to simulate the dynamics of mean stage and storage in a reach, and the resulting time series of outflow Q:

$$\begin{cases} \dfrac{dS(t)}{dt} = I(t) - Q(t) \\[2mm] Q(S) = \dfrac{S - k(S) \cdot x \cdot I}{k(S)(1-x)} \\[2mm] k(S) = \dfrac{L \cdot n}{s_o^{1/2}} \cdot \left[\dfrac{L \cdot T^2 + 2 \cdot S}{T \cdot S} \right]^{2/3} \end{cases}$$

This method is applicable to various river flow conditions. More importantly, it can easily be generalized to other river bed geometries by modifying the hydraulic radius equation as Eq. (3-7), (3-8), (3-9).

4. Numerical method

When the two studied methods, Muskingum and M-M method, are applied into practice, one of the most important thing is how to integrate the storage in the reach from one time step to the next, because the flow routing mainly depends upon the dynamics of storage. This section deals with the choice of an efficient numerical method to perform the required integration over time. We considered two explicit finite difference methods, the Euler and fourth-order Runge-Kutta methods, and tested them in the case of the Muskingum scheme, but the results are completely transferable to the Muskingum-and-Manning equation, as the dependence of k on S is straightforward with an explicit scheme.

4.1 Basic concept in numerical method

4.1.1 Finite difference

A finite difference is like a differential quotient in mathematics, except that it uses finite quantities instead of infinitesimal ones. In numerical analysis, especially in numerical ordinary differential equations and numerical partial differential equations, finite differences is used to approximate derivatives, which aim at the numerical solution of ordinary and partial differential equations respectively. [Maidment, 1993]

In this study, we could get the storage variation within the timestep with the known inflow and the outflow as in Eq. (2-3). This equation indicates a simple function of storage as following:

$$\frac{dS}{dt} = f(S) \tag{4-1}$$

The function f(S) is defined as below in the Muskingum case:

$$f(S) = I(t) - Q(t) = I(t) - \frac{S(t) - k \cdot x \cdot I(t)}{k \cdot (1-x)} \tag{4-2}$$

Integrating this derivative with a small embodied timestep Δt, the difference of storage dS in Eq. (4-1) can be expressed by S(t+Δt)-S(t):

$$\frac{S(t + \Delta t) - S(t)}{\Delta t} = f(S) \tag{4-3}$$

Eq. (4-3) is called a finite-difference equation of storage S. Solving this equation gives an approximate solution of the storage value defined by the differential equation.

The error between the approximate solution and the true solution is determined by the error that is made by going from a differential operator to a difference operator. This error is called the discretization error or truncation error (the term truncation error reflects the fact that a difference operator can be viewed as a finite part of the infinite Taylor series of the differential operator).

4.1.2 Explicit method

In applied mathematics, explicit method is an approach used in computer simulations of physical process, or in other words, it is a numerical method for solving time-variable ordinary and partial differential equations.

Explicit methods calculate the state of a system at a later time from the state at the current time using a forward difference. In Eq. (4-3), if S(t) is the current system state and S(t+Δt) is the state at the later time, then we can get the explicit method for solving the one-dimensional storage equation:

$$S(t + \Delta t) = f(S(t), \Delta t) \tag{4-4}$$

So, knowing the storage value at time t, the corresponding storage value at time t+Δt can be obtained by using this relation.

4.2 Two explicit schemes

4.2.1 Euler method

The Euler method advances a solution from time t to next time t+Δt, which is the most simple combination of Eq. (4-3) and Eq.(4-4). Hence the formula for calculating the storage is:

$$S(t + \Delta t) = S(t) + \Delta t \cdot f(S(t)) + O(\Delta t^2) \tag{4-5}$$

This formula means that the solution is advanced through an interval Δt. It uses the obtained information derived from Eq. (4-3) only at the beginning of that interval. The step's error $O(\Delta t^2)$ is only two powers of Δt.

4.2.2 Fourth-order Runge-Kutta method

Consider the use of a step like Eq. (4-4) to take a "trial" step to the midpoint of the interval. Then use two values at that midpoint to compute the "real" step across the whole interval. By using the initial derivative at each step to find a point halfway across the interval, then using the midpoint derivative across the full width of the interval, the accuracy can be improved. That is the basic idea of the Runge-Kutta method, which is a bit more sophisticated and supposedly much more efficient than the Euler method, i.e. providing a much better precision with only a few additional operations. The classical fourth-order Runge-Kutta method (abbreviated RK4 in the following) is brought out based on this idea using four intermediate estimations. To integrate Eq. (4-3), which describes the storage variations, in case of the Muskingum or Muskingum-Manning schemes depending on the form of function, the RK4 method can be expanded as follows:

$$\left\{ \begin{array}{l} k_1 = \Delta t \cdot f(S(t)) \\[2mm] k_2 = \Delta t \cdot f(S(t) + \dfrac{k_1}{2}) \\[2mm] k_3 = \Delta t \cdot f(S(t) + \dfrac{k_2}{2}) \\[2mm] k_4 = \Delta t \cdot f(S(t) + k_3) \\[2mm] S(t + \Delta t) = S(t) + \dfrac{k_1}{6} + \dfrac{k_2}{3} + \dfrac{k_3}{3} + \dfrac{k_4}{6} + O(\Delta t^5) \end{array} \right.$$

The RK4 method is mathematically proper, since any point along the trajectory of an ordinary differential equation can serve as an initial point. In this method, in each step the derivative is evaluated four times: once at the initial point, twice at trail midpoint, and once at a trail endpoint. From these derivatives the final function value is calculated and the step's error $O(\Delta t^5)$ is five powers of Δt. The fact that all steps are treated identically also makes it easy to incorporate it into relatively simple "driver" schemes. [Press et al. 1992]

For each integration timestep, RK4 method uses four operations where Euler method only uses one, but the error is three orders of magnitude smaller.

4.3 Comparison of performances with respect to precision

We compared the above two numerical methods, the Euler and RK4 methods, to compute the storage through one day in a simple reach with Muskingum method.

For the purpose of obtaining the daily outflow and compare results to conclude which method is more precise during one day, we compared different time step to subdivide one whole day. Q at end of one integration timestep can be derived from the calculated storage value, which is updated and serves as initial condition for the following timestep. Here are the different values that were compared in this study: $\Delta t = 24$ h, $\Delta t = 12$ h, $\Delta t = 6$h, $\Delta t = 1$ h, $\Delta t = 20$ min and $\Delta t = 1$ min.

To better examine the computational results, these two methods are applied with the different time steps in multiple situations. These situations, involving diverse values of initial storage S(0), inflow I assumed constant all day long, and different values of the Muskingum parameters k and x, is shown in Tab. 4-1. In this table, the selected values of k induce mean velocities ranging from almost 0 up to 5.8 m/s with reach length of 1 km and to 579 m/s for a reach of 100 km, widely encompassing typical riverflow velocities which are between 0.1 and 1m/s in most cases.

Table 4-1. Multiple situations for application

Case	k (days)	S(0) (m³)	I (m³/s)	x	v_e (m/s)		
					L=1km	L=10km	L=100km
I	**0,002**	10	10/86400	0 / 0,5	5,7870	57,8704	578,7037
II	**0,02**	10	10/86400	0 / 0,5	0,5787	5,7870	57,8704
III	**0,2**	10	10/86400	0 / 0,5	0,0579	0,5787	5,7870
IV	**0,7**	10	10/86400	0 / 0,5	0,0165	0,1653	1,6534
V	**2**	10	10/86400	0 / 0,5	0,0058	0,0579	0,5787
VI	2	**500**	10/86400	0	0,0058	0,0579	0,5787
VII	2	**1000**	10/86400	0	0,0058	0,0579	0,5787
VIII	2	10	**6/86400**	0	0,0058	0,0579	0,5787
IX	2	10	**50/86400**	0	0,0058	0,0579	0,5787
X	**8**	10	10/86400	0 / 0,5	0,0014	0,0145	0,1447
XI	**20**	10	10/86400	0 / 0,5	0,0006	0,0058	0,0579

Fig. 4-1 describes the relationship between reach length L, k and the mean flow velocity v_e in Eq. 3-2 transforming certain velocity to the value of k.
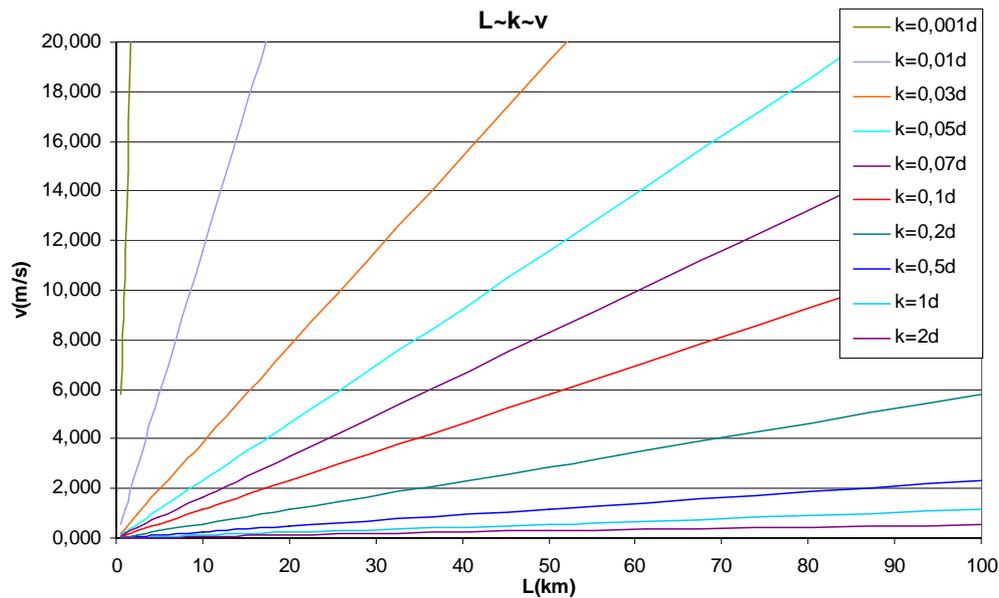
Figure 4-1. The normal relationship between reach length, k and velocity

Given the constant inflow I and Muskingum parameters k, the initial storage S is advanced by the Euler and RK4 numerical methods, and then the final storage is obtained and compared in appendix 1. The result is the most precise when Δt = 1 min. Given this reference, Fig. 4-2 shows that the smaller the timestep, the more precise the result of final storage. And the calculations of RK4 method presented by blue polylines are always more accurate than that of Euler method which is presented by pink polylines. These conclusions hold in all tested situations (Table 4-1), as shown in appendix 1. The relative errors in final storages are also analyzed respectively in appendix 2 with different parameters.
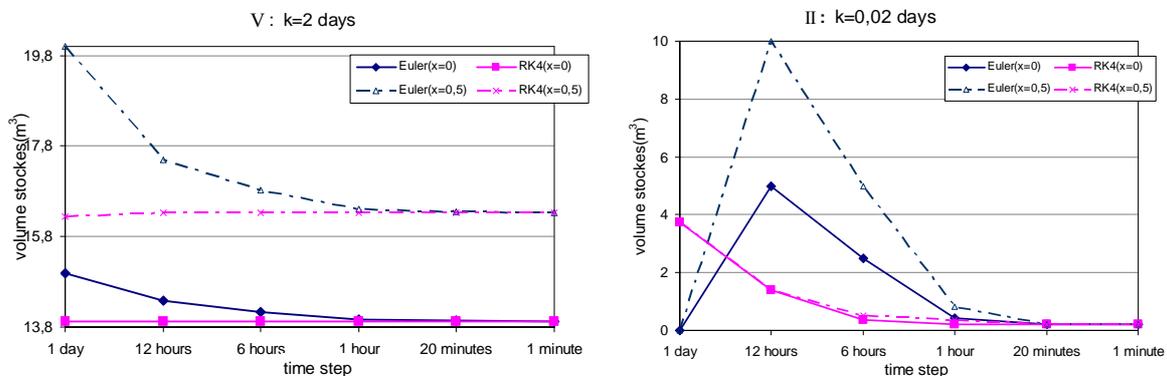
Figure 4-2. Calculation results of Euler and RK4 numerical methods in different situation

Not surprisingly, this analysis shows the smaller is the timestep, the higher the precision. It also shows that the optimum timestep (largest precise timesteps) is different with the two methods. With the Euler method, we need Δt = 20 min in to achieve a precise result. With the RK4 method, a similar precision is reached up to Δt = 6h.

4.4 Conclusion for numerical method and timestep

By comparing the computational results of Euler method and RK4 method, we can get the following conclusions:

♦ The RK4 method with the time step Δt = 6h obtains a precise result in all the tested situations, widely encompassing the typical river flow velocities.

♦ To obtain a similar precision, the Euler method must be used with a much smaller timestep, Δt = 20 min.

♦ The required number of operations to achieve the same precision over 1 day is 4×4=16 for RK4 and 3×24=72 for Euler.

So in this study, we chose to integrate both routing methods, the Muskingum and M-M methods, using the RK4 method with a time step of Δt = 6h.

4.5 Negative initial outflow in Muskingum method

Perumal [1992] mentioned that the Muskingum method has the problem of negative or reduced initial outflow and he inferred that this may be explained by a consideration of a linear variation of discharge along the reach and by a linear extrapolation of the weighted discharge $Q_w(t)$ shown in Fig. 4-3:
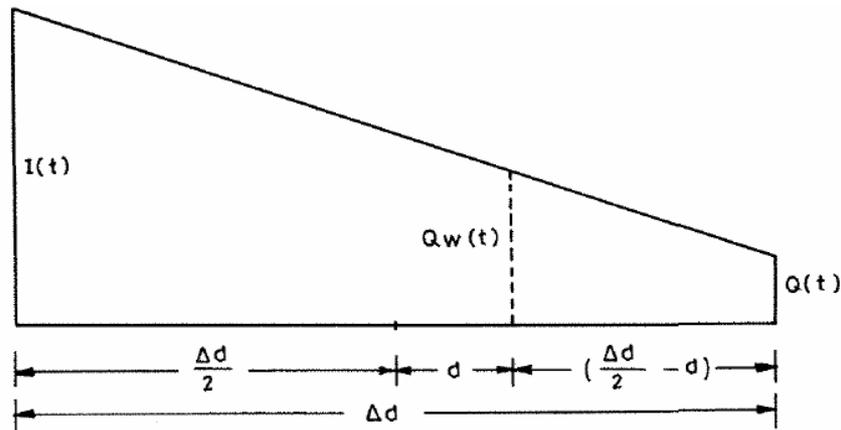
Figure 4-3. Schema of the weighted discharge $Q_w(t)$ [Perumal,1992]

Where the weighted discharge $x \cdot I(t) + (1 - x) \cdot Q(t)$ be denoted by $Q_w(t)$.

The relation equation between outflow Q(t), inflow I(t) and the weighted discharge $Q_w(t)$ is as below:

$$Q(t) = -\frac{x}{1-x} \cdot I(t) + \frac{Q_w(t)}{(1-x)} \qquad (4-6)$$

Where the Muskingum parameter x is regarded as the distance proportion $x = \frac{\Delta d/2 - d}{\Delta d}$.

Hence it may be inferred from Eq. (4-6), that when $x \cdot I(t) \leq Q_w(t)$, then $Q(t) \geq 0$; the outflow $Q(t) < 0$ only when $x \cdot I(t) > Q_w(t)$.

In this study, the problem of negative initial outflow has been concerned. To prevent from this simulation, the inflow I(t) or the x takes the value which is high enough to cause $x \cdot I(t) > Q_w(t)$, then we take the shorter timestep to get the precise result of inflow which is smaller than the results by the longer timestep. That is to say, the smaller value of inflow I gotten by shorter timestep can avoid the problem of negative outflow. So the Muskingum method can work better with shorter timestep. We also give an upper limit in calculating the outflow to insure it not to be negative, which is describe in Sec. 5.1.1 (P. 19).

5. Application of two routing methods

The main objective of the two tested models is to estimate the flow routing transformation and water volume stored in the different reaches composing the river network.

The Muskingum and M-M methods have been first applied in a simple reach. The simulation results were shown to be correct and efficient. So the study develops from one simple reach to a complicated river network.

5.1 Sensitivity in different situations in a reach

Before applying the method to a natural river network, many situations were considered to ascertain the validity and robustness of the tested routing schemes. If some routing factors change, it may influence all the simulations as well as the results.

Three representative situations are given in Tab. (5-1) to apply the routing models, which are named as "rising to a steady mode", "pulse" and "pure recession".

♦ "Rising to a steady mode" means that the initial storage in the reach is almost empty, the inflow is constant, the outflow increases up until it equals the inflow in a steady state with constant storage.

♦ In the "Pulse" situation, we consider a pulse inflow, during the first timestep of the simulation, then inflow is zero and we look at the transfer of this unit inflow through the reach.

♦ "Pure recession" is another characteristic situation. The initial storage in reach is not zero and we study the recession dynamic of this store in absence of inflow, until it ends up being totally empty.

Table 5-1. Different situations for routing simulation

Case	Name	I (m³/s)	Initial S (m³)
I	Rising to a steady mode	x	0
II	Pulse	$I(t=1) = x$ and $I(t>1) = 0$	0 or y
III	Pure recession	0	y

x is a constant value of inflow discharge, x>0; y is a value of initial storage in reach, y>0 too.

The results are shown in appendix 3 for the two tested routing schemes: the Muskingum method and M-M method, both with the RK4 method and Δt =6h. The difference between them is whether the Muskingum coefficient k is constant or not.

5.1.1 Muskingum method

In Muskingum method, k determines the speed of river flow. The larger k, the smaller the flow velocity, and the slower the outflow rise to the steady mode. The other coefficient x

describes the attenuation of the wave. We can see that in "rising to a steady mode" with Δt=6h in Fig. 5-1(left), the steady discharge smaller than expected for the smallest k or fastest flow (k=0.11day), and that for the second smallest k (k=0.57day), there is oscillations of outflow discharge around the steady state.
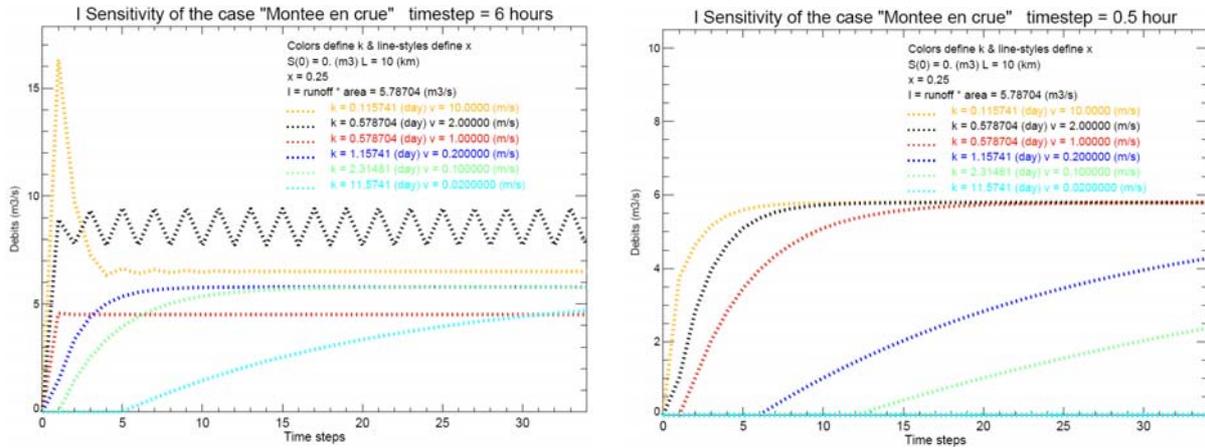
Figure 5-1. Sensitivities with different k for Δt = 6h (left) and for Δt = 0.5h (right)

In the conservation equation (2-3), the variation of storage par time step is equal to the difference between inflow and outflow:

$$\frac{S(t + \Delta t) - S(t)}{\Delta t} = I(t) - Q(t) \qquad (5\text{-}1)$$

In our code, to insure that S(t+Δt) ≥ 0, Q(t) has been bounded with respect to the following upper limit:

$$Q(t) \le I(t) + \frac{S(t)}{\Delta t} \qquad (5\text{-}2)$$

This was completed in our program as follows:

$$Q(t) = \min\left[\frac{S(t) - k \cdot x \cdot I(t)}{k \cdot (1 - x)}, \ I(t) + \frac{S(t)}{\Delta t} \right] \qquad (5\text{-}3)$$

Therefore, when the calculated Q(t) is higher than the upper limit, Eq. (5-3) reduces Q(t) to a lower value. This leads to the lower steady discharge shown by yellow curve in Fig. 5-1(left). The oscillations of black curve are also caused by this limit of outflow, which reduces the outflow sporadically when Q(t) gets higher than the limit.

The above upper limit depend on Δt, and we tested if we could correct our simulation from the above problems with a shorter timestep than Δt = 6h. Fig. 5-1(right) shows the results of the simulation using Δt = 0.5h, which represents the good simulation without any oscillations. Hence, shorter timesteps lead to more precise results as expected.

5.1.2 Muskingum-and-Manning method

In the M-M method, k is no longer constant and it depends on the morphology of the reach (i.e.T, L, n, s_0), and on storage or water stage, which was one goal of the method. The coefficient x still determines the form of the flow curve. If most simulations were consistent with theory, we highlighted some questionable behaviour.

The initial peak of discharge in the situation "Rising to a steady mode" with x=0.5 (P.35) has a numerical origin, as the outflow discharge is limited to avoid negative storage. And some undulate phenomenon of discharge when simulating with different lengths in "Rising to a

steady mode" are also the results of this limit. This has been discussed in Sec. 5.1.1. These features would disappear if we take a smaller timestep. Fig. 5-2 give an example of the solution.

In the results of k, the nearly vertical part corresponds to an infinite k when the storage is zero in reach. In such a case, outflow is zero.

We also found that the variations of slope or length of reach can produce different value of the steady state of discharge, as shown for example in Fig. 5-2 (left). By studying the relationship between storage, k, and physical channel characteristics (length L, width T, roughness of Manning n and riverbed slope s_o) described in Fig. 5-3, 5-4, 5-5, 5-6, which shows that to certain value of reaches' characteristics, there is one single value of storage. So the feature of different value of steady state in Fig. 5-2 (left) is the numerical problem caused by the upper limit in Eq. 5-3. If we take the shorter timestep (Δt = 1h), this problem is well solved, in Fig. 5-2 (right).
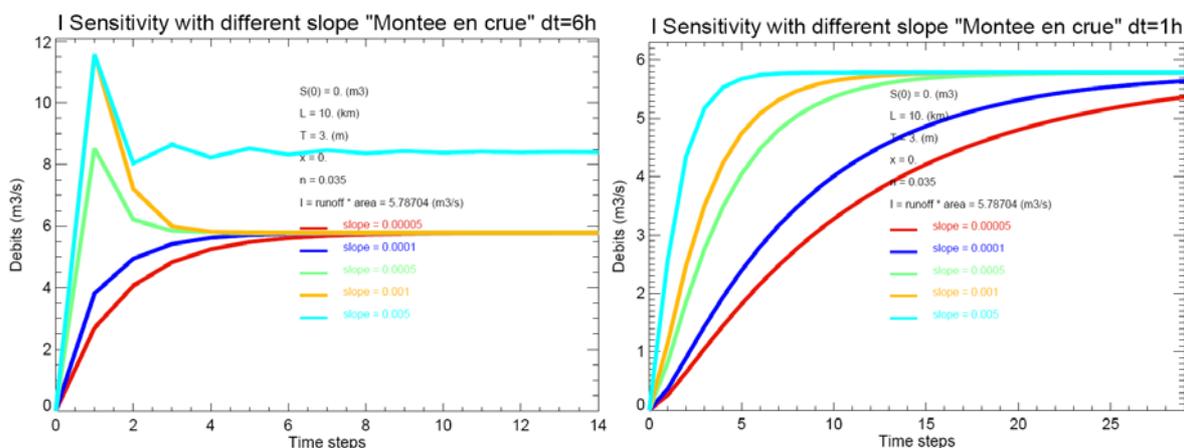
Figure 5-2. Sensitivities of discharges with different slope using Δt = 6h (left) and Δt = 1h (right)
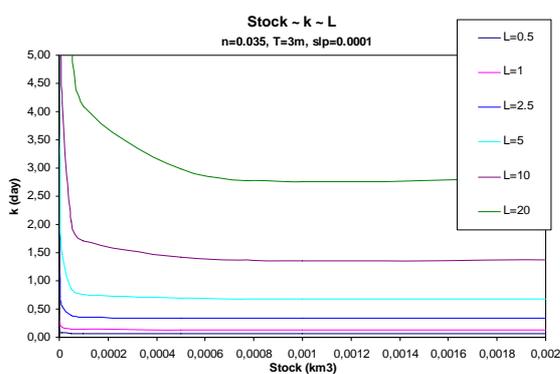
Figure 5-3. The relationship between storage, k and reach length (m)
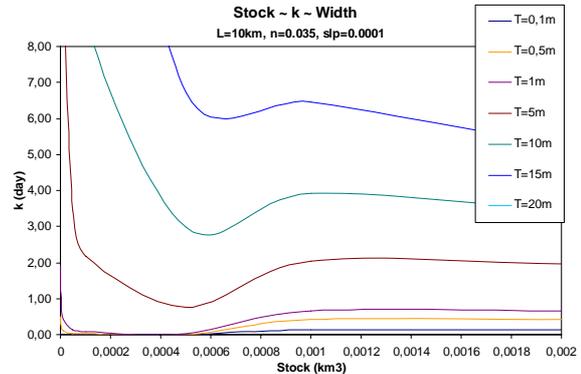
Figure 5-4. The relationship between storage, k and reach width (m)
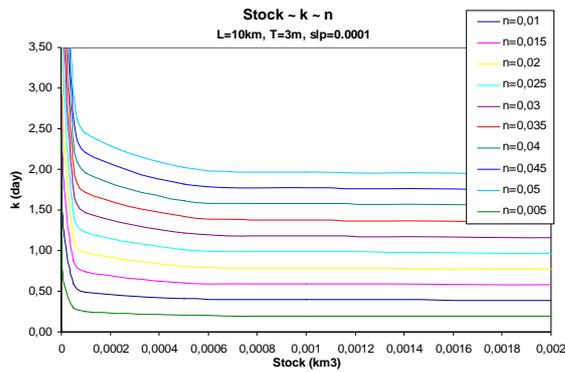
Figure 5-5. The relationship between storage, k and Manning's n (-)
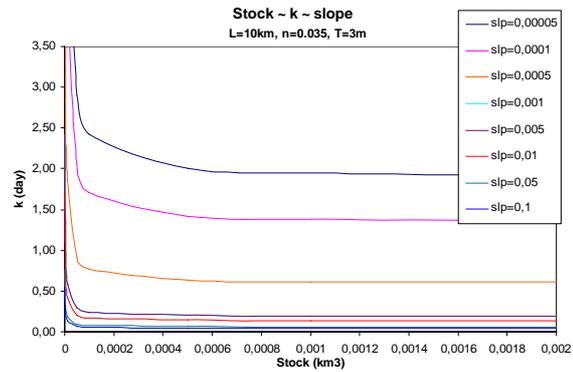
Figure 5-6. The relationship between storage, k and reach slope(-)

Generally to say, when Manning' roughness n increases, the flow discharge is slower; when the slope increases, the flow is faster; when the reach length increases, the flow is slower; when river width increases, the flow is slower. This can turn out to be the opposite when the conditions impose the upper bound for mass conservation, but this inaccuracy can be solved buy using a smaller timestep.

5.1.3 Conclusion for simulation in a reach

From the application with the Muskingum method and M-M method and their sensitivities of diverse parameters, it is concluded that these two methods could both commendably simulate the flow routing in a simple reach. The latter can integrate the linear reservoir model and variable parameter together to better simulate the dynamic natural flow. In the various sensitivity tests, we mostly got the results that were expected, and we could propose simple solutions to overcome the diagnosed problems, which show that the code is correctly designed.

5.2 Sensitivity in a theoretical river network

5.2.1 Construction of the river network

A hypothetic river network was built with four levels of reach, the level increasing at each confluence (as in the Strahler ordering scheme), from 0 in the upstream reached to 3 in the downstream reach. At level 0, we do not consider any storage in the river reaches, i.e. the runoff accumulated over the timestep is totally discharged at the outlet of the basin at the end of the timestep and contributes to the inflow of the reaches of level 1. The reaches of level 1, level 2 and level 3 have two contributing reaches. They can store water in the reach during the routing, and the outflow from a reach of level n contributes to the inflow of the downstream reach of level n+1, which allows for the routing along the network. Here is the scheme of the river network (Fig. 5-7).

In the following results, all the reaches have the same morphology (L, T, n, s_o, rectangular shape) and Muskingum parameters (k and x).

We defined four forcing situations (Tab.5-2). The first three ones are a generalization of the ones tested in a simple reach to all the reaches of the network, so that all the reached have the same runoff forcing for a given timestep. The fourth situation, named "Pulse upstream", is designed to assess a non uniform forcing. It consists of the "pulse" forcing in all the upstream reaches of level 0, with no runoff downstream, from level 1 to level 3. This situation allows us to study the routing of a flood wave generated in a fraction of the watershed, here the most upstream fraction.

21
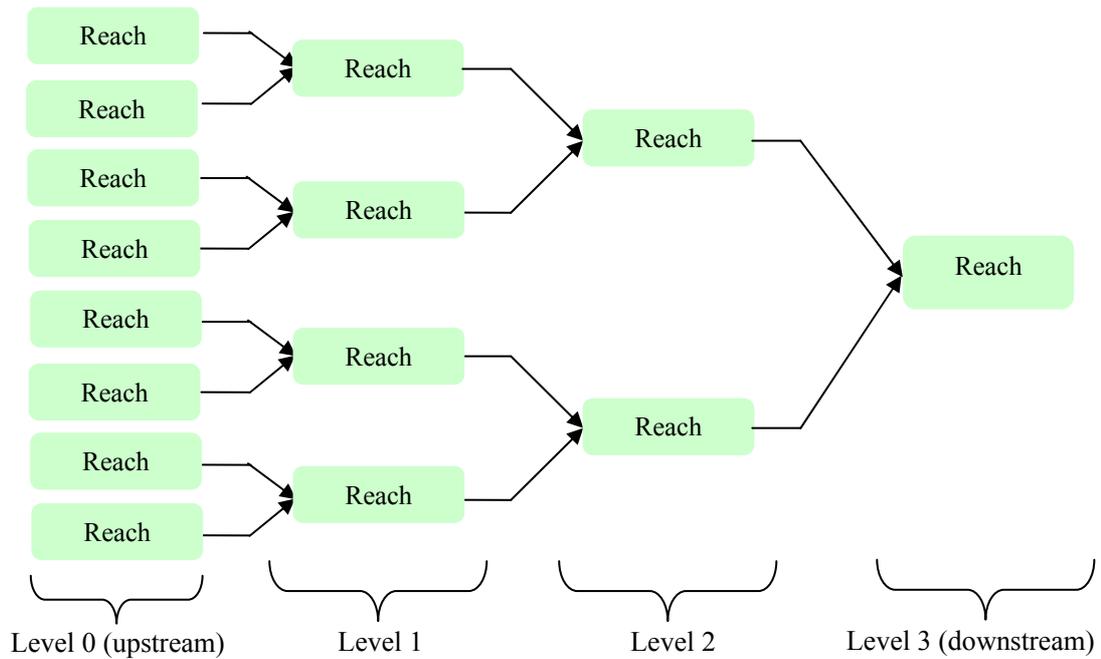
Figure 5-7. The scheme of the theoretical river network

Table 5-2. Different situations for routing simulation in river network

Case	Name	I (m^3/s)	Initial S (m^3)
I	Rising to a steady mode	x	0
II	Pure recession	x	y
III	Pulse	I(t=1) = x and I(t>1) = 0	0 or y
IV	Pulse upstream	I(t=1) = x (level=0) and I(t>1) = 0 (other levels)	0 or y

Here x and y are same as those in table 5-1.

As in a unique reach (Sec. 5.1), we studied the sensitivity of the two routing models to their different parameters (k and x for Muskingum method, and x, T, L, n and s$_o$ for M-M method). The results of these simulations are presented in appendix 4 and are discussed below.

Note that in the situation "Pure recession", we start from a state where all the reaches are at a steady with respect to their runoff input. But at levels 1 to 3, the inflow from the upstream reaches induces an increase in discharge and storage. So the river network itself is not in a steady state.

5.2.2 Muskingum scheme

In Muskingum method, there are always two parameters to be analyzed: k and x. As in the simple reach, the k and x determine the rising speed and the shape of the curve of flow series.

With the Muskingum method and the situation of "Pulse" and "Pulse upstream", the results obtained with the minimum value of k (k=0.23day) are exceptional to the others (for example, the situation of "Pulse" in Fig. 5-8 (left)). The integrated discharge over the simulation is smaller than in the other cases. That is to say when the river flow gets slower it will lead to an

incorrect computation result. Again, the reason is the upper limit imposed on discharge (Eq. 5-3).

To prevent the use of the second term $I(t) + \dfrac{S(t)}{\Delta t}$ as an upper limit in Eq. (5-3), we need that:

$$\frac{S(t) - k \cdot x \cdot I(t)}{k \cdot (1 - x)} \leq I(t) + \frac{S(t)}{\Delta t} \tag{5-4}$$

So it is necessary that the method's application with the situation of "Pulse" and "Pulse upstream" should conform to the following condition:

$$\Delta t < k \cdot (1 - x) \tag{5-5}$$

In other words, the maximum time step Δt in each river reach varies with k and x. So this method can be generally applied to the broad and long rivers, with rather slow flow (high k). If we come across the same problem in practice, we should take a smaller time step to satisfy the above condition (In our case "Pulse", the timestep should be smaller than 2.778 hours, so we calculate the outflow with $\Delta t = 2h$), and we could easily use it as a preliminary check before running a simulation. Fig. 5-8 (right) shows the good simulation using the shorter timestep.
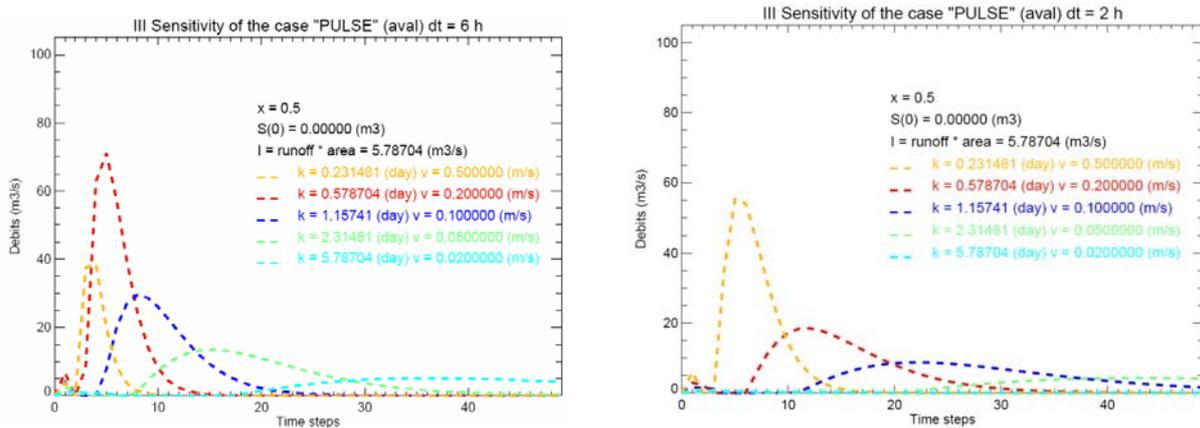
Figure 5-8. Sensitivities with "Pulse" using $\Delta t = 6h$ (left) and $\Delta t = 2h$ (right) with different k

5.2.3 Muskingum-and-Manning scheme

The simulations of this method in the hypothetic river network are consistent with what was simulated in a unique reach, thus the unusual peak in discharge when river width T = 10 m is not as expected to be smaller than T = 5 m. This is well illustrated in the "Pulse upstream" situation (Fig. 5-9). We know that a larger storage induces a larger discharge and a larger width induces a slower velocity. After adapting the smaller timestep($\Delta t=4h$), the peaks are smoothed for T=5 to 20m, and the maximum discharge is smaller for T=10m than for T=5m, as expected. So this is again a numerical problem. The sensitivities of other parameters are similar to the results which have been summed up in the application of this method in a simple reach.
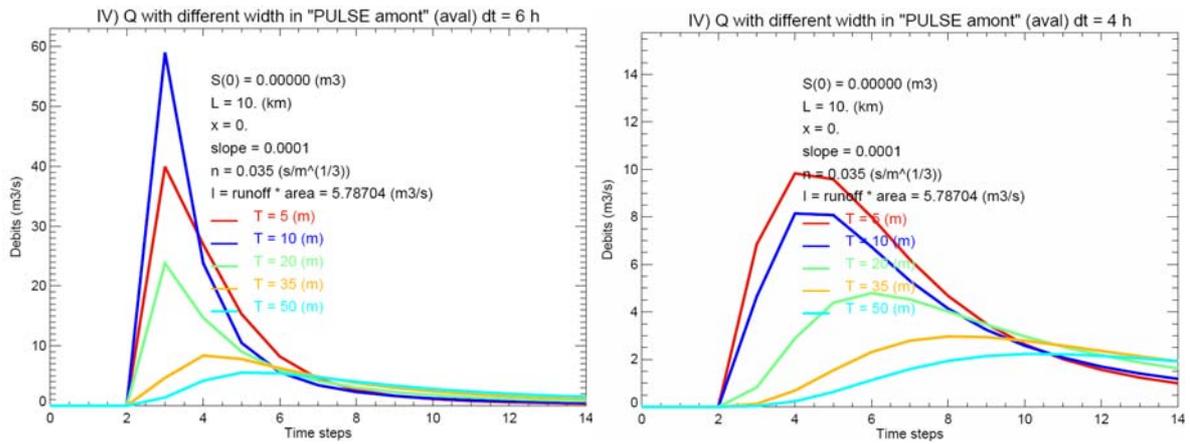
Figure 5-9. Sensitivities with "Pulse upstream" with different T for Δt = 6h (left) and for Δt = 4h (right)

5.2.4 Conclusion for simulation in a river network

In this section, the Muskingum and Muskingum-and-Manning methods are applied in a hypothetical, regular river network. The variable value of k plays a great part in the whole simulations, which is influenced by many parameters: reach length, width, slope, Manning's roughness and the storage. If one of these parameters changes, it will cause the k variable. Just like a chain which can transmit the information, it links the flow routing and river's factor to be related together.

6. Application in the Seine River basin

6.1 Seine River basin

By French standards, the Seine river basin is highly populated: the watershed covers only 12% of the French territory but hosts 25% of its population. But the population is not uniformly distributed within the basin: 10 of the 17 millions inhabitants are living on less than 4% of the watershed (Paris urban area). As a result, population density along the river can vary from 3 to 5000 people per km^2. Human pressure in river corridors is among the highest in Europe, not only in Paris, but also near some midsize cities (Reims, Beauvais…).[Kieken, 2000] Otherwise the Seine river has the most sinuous course of all French rivers, especially between Paris and the Channel. Its main tributaries are the Aube, the Yonne, the Loing, the Essonne, the Eure, the Marne, the Aisne, and the Oise which has its source in Belgium (Fig. 6-1). Consequently, it would be very useful to be able to simulate flooding.
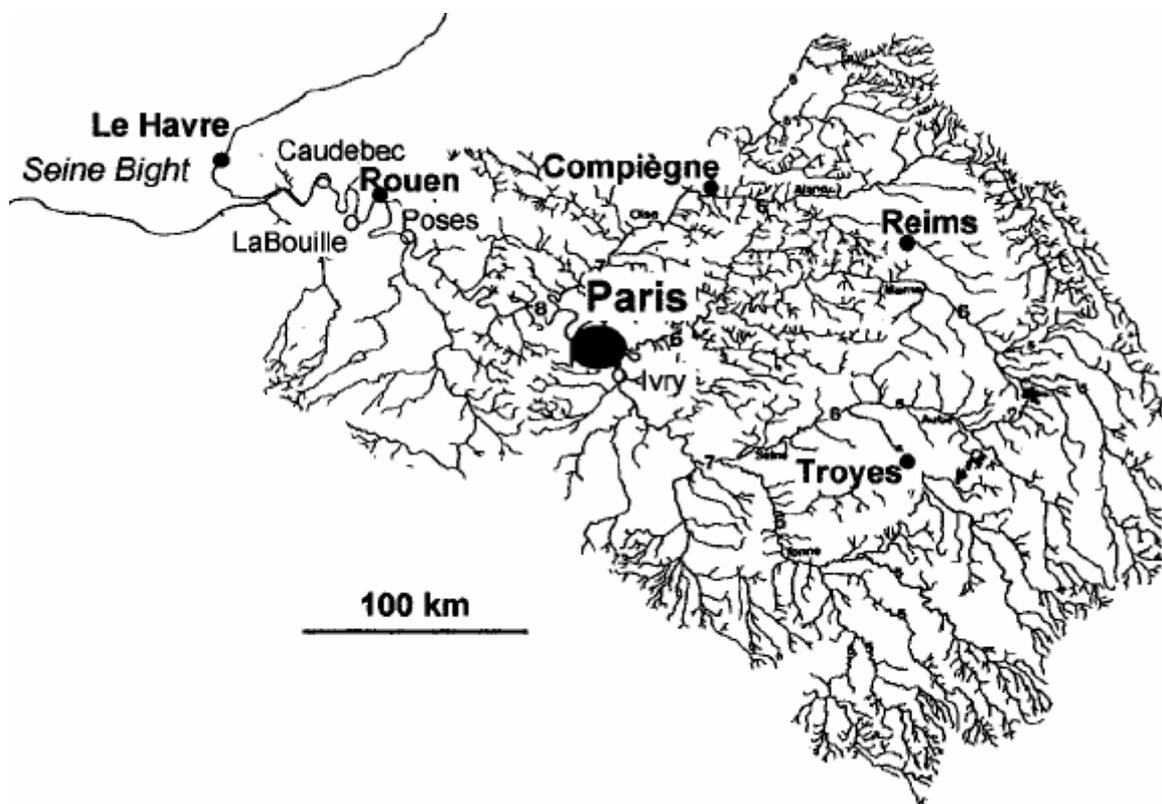
Figure 6-1 Hydrographical network of the basin of Seine [Billen et al, 2001]

6.2 The land surface model (CLSM)

The catchment-based land surface model [CLSM; Koster et al., 2000 and Ducharne et al., 2000] provides a physically based description of the influence of climate on runoff. As a land surface model (LSM), it is designed to simulate the diurnal cycle of land surface water and energy fluxes as a function of near-surface meteorology (precipitation, short-wave and long-wave incident radiation, surface pressure, air temperature and humidity at 2 m, wind speed at 10 m) and can either be coupled to a GCM or used off-line as in the present study. The CLSM belongs to a new generation of LSMs which rely on the concepts of the hydrological model TOPMODEL to account for lateral water fluxes along topography, their influence on the

24

small scale variability of soil moisture, runoff and evapotranspiration, thus on larger scale water budget. [Ducharne et al, 2007]

For this study, the CLSM model is used to get the runoff in mm/h throughout the network. The Seine watershed upstream Poses was subdivided into 27 unit catchments, with an average size of 2600 km2. Catchment delineation and topographic index computation were based on a 100-m resolution DEM. In each unit-catchment, the vegetation and most soil properties (depth, porosity, wilting point, matric potential at saturation, Clapp and Hornberger's parameter b) were derived from the 1-km ECOCLIMAP database [Masson et al., 2003]. The two parameters describing the vertical profile of saturated hydraulic conductivity, namely the saturated conductivity at the surface and its vertical decay factor, were calibrated.

A reference simulation was performed over six years (August 1985–July 1991) using this set-up and observed meteorological forcing at a 1-hour and 8-km resolution. The CLSM does not account for the routing of runoff into streamflow and discharge is approximated by the spatial mean of runoff over 10 days (close to the concentration time of watershed). Corrected for the influence of three large regulation reservoirs in the upstream part of the watershed, it compared satisfactorily with observed streamflow in 20 gauging stations at the 10-day timestep. The Nash efficiency ranges from -0.1 at Courlon-sur-Yonne to 0.86 at Vitry-en-Perthois (Saulx), and reaches 0.81 at Paris and 0.67 at Poses. The interannual variability of floods is realistically simulated, but low flows are not sustained enough, especially in the central and western areas where significant aquifers are connected to the river.
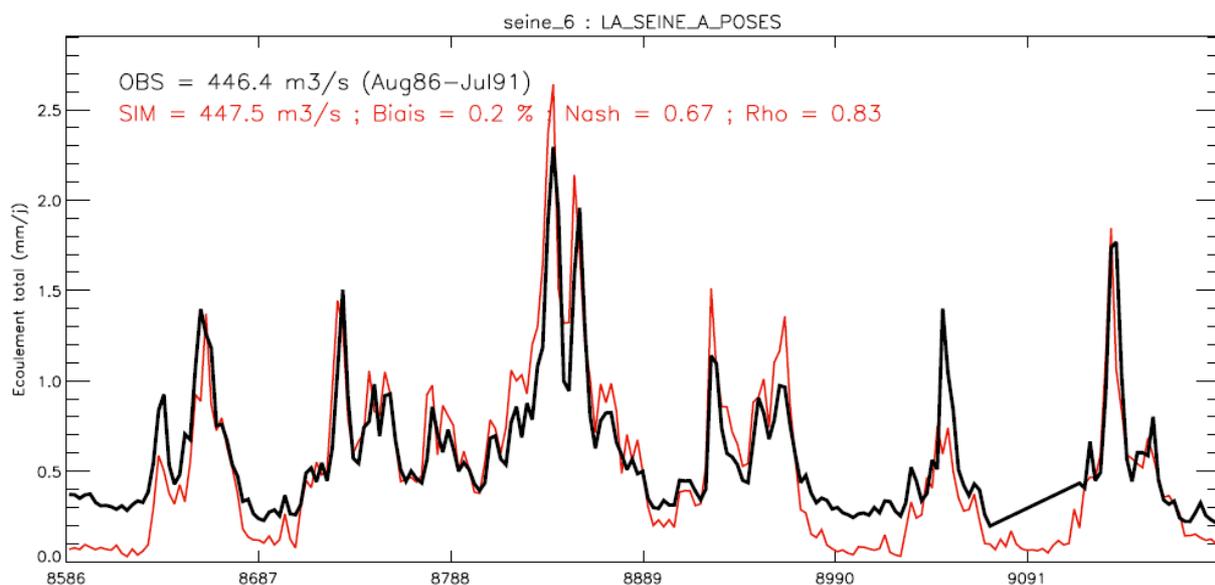
Figure 6-2. Comparison between observed and simulated discharge at the outlet of the Seine

6.3 Characteristics of the basin from GIS

To simulate of flow routing, the physical characteristics of the stream reaches in each unit-basin are required to compute the variable parameter k. There are 29 sub-basins in the Seine basin according to the CLSM. We distinguish 15 head basins where the transformation of runoff into river is instantaneous, and 14 basins, where we want to simulate the routing of river flow in the main reach.

Here with the help of Geographic Information System (GIS), it has been very convenient to get the Seine basin's characteristics. The main distribution of all the sub-basin is obviously shown in Fig. 6-3. The black boundaries divide the Seine into 29 sub-basins. The 15 sub-

basins upstream are distinguished by using the red interlaced lines, which present all the rivers in these sub-basins, from the colorized-lines regions. In these upstream sub-basins, we will not account for routing in a first step, thus only the runoffs and areas of sub-basins are. As for the other sub-basins, besides the runoffs and the areas, it is also necessary to characterize the physical characteristics of the mainstream of each sub-basin, the average width T and average slope so and the length L from the inlet to the outlet of mainstream, which can be obtained by GIS. As an example, Fig. 6-4 shows in blue the mainstream of the Oise in the the lower sub-basin Oise_2, where the simulated flow from the upstream sub-basins, Oise_a and Aisne will be routed.
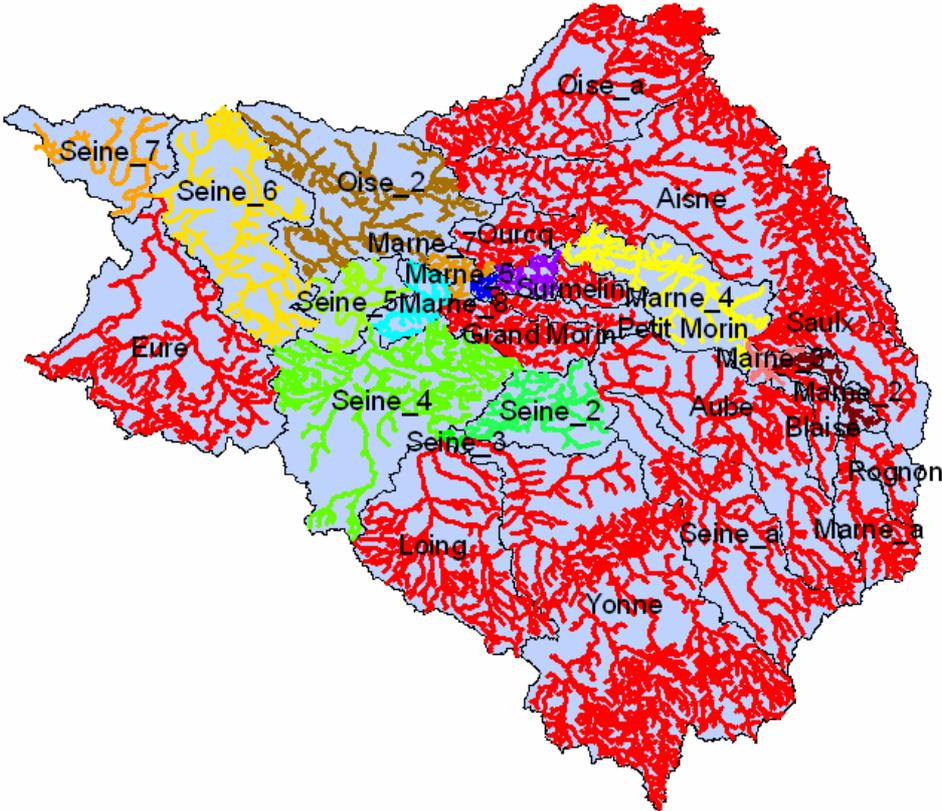
Figure 6-3 Hydrographical network of the basin of Seine
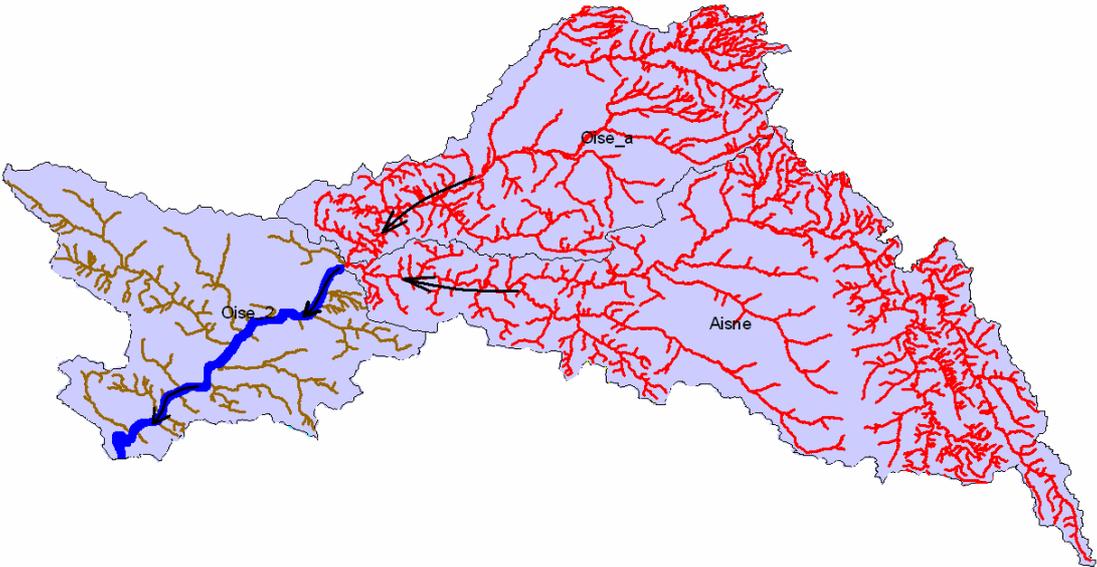
Fig. 6-4 Flow routing from the upstream sub-basin (Oise_a and Aisne) to lower sub-basin (Oise_2)

6.4 Flow routing simulation

In the process of the flow simulation in Seine, the model CLSM will give runoff to be routed as discharge using the M-M scheme and the RK4 method with timestep is 6h. The Manning coefficient of roughness, n, is fixed to be the global value: $n = 0.035$ s/m$^{1/3}$, and the weighting factor of Muskingum method, x, is set to be the minimum value, x=0, for a first trial.

Within 15 headwater basins (signed with red river lines in Fig. 6-3), the 6h outflow will in first approximation be deduced from the simple accumulation of runoff over the basin during the timestep. River flow routing will be performed in the 14 remaining basins, using the above outflow as inflow. The 6h accumulation of runoff from each of the 14 basins will be added at each timestep as lateral inflow in the corresponding river store without any transformation. The parameters of the M-M scheme will be deduced from the morphology of the main reach.

We have been lacking for the runoff results derived from the CLSM simulation until this thesis is completed. Hence the simulation result in Seine River basin is not reached and this work is left to be continued in the future.

7. Conclusion

The classical routing Muskingum method was combined with the Manning equation to simulate the natural flow routing in a basin in this study.

By applying this Muskingum-and-Manning method in a simple reach and in a hypothetic regular river network, the results rightly reflect the influence of different parameter of hydrological conditions and of the shape as well as the roughness degree of the river bed. This method shall be tested in the Seine river network, in combination with the runoff simulated by the Catchment-based LSM.

From our study, the conditions to guarantee a good simulation of Muskingum-and-Manning method are summed up as following:

(1) The numerical integration method, RK4 method is preferable than the Euler method.

(2) The timestep $\Delta t = 6h$ is not sufficient in some of the tested cases, when flow is fast (i.e. small T, small k, small L) especially with high x.

(3) The timestep $\Delta t < 6h$ is more feasible.

(4) When the inflow is zero, I(t)=0, the limit of timestep is $\Delta t < k \cdot (1 - x)$.

(5) Once the numerical problems are settled, the Muskingum-and-Manning method can describe correctly the water depth and its influence on discharge.

Developing a good applied method for river flow routing simulation is still one important research subject. The prospects are numerous from LSM validation, to the hydrology forecast or the design of hydrological works. So the method proposed in this study has some practical sense and it remain to be tested in the non-theoretical case. It will be further validated and developed in the future.

Bibliography

[1] Akgiray, Ö. (2005), Explicit solutions of the Manning equation for partially filled circular pipes, Canadian Journal of Civil Engineering, Eng. 32, 490-499.

[2] Arora, V. K., Chiew, F. H. S., and Grayson, R. B. (1999), A river flow routing scheme for general circulation model, Journal of geophysical research, Vol. 104, No. D12, 14,347-14,357, Jun. 27.

[3] Arora, V., Seglenieks, F., Kouwen, N., and Soulis, E. (2001), Scaling aspects of river flow routing, Hydrological processes, 15, 0000-0000.

[4] Arora, V. K., and Boer, G. J. (1999), A variable velocity flow routing algorithm for GCMs, Journal of geophysical research, Vol. 104, No. D24, 30,965-30,979, Dec. 27.

[5] Bathurst, J. C. (1988), Flow processes and data provision for channel flow models, in Modelling geomorphological systems, Anderson, M. G. Eds., Wiely, Chichester, pp 127-152.

[6] Becker, A., and Serban, P. (1990), Hydrological models for water-resources systems design and operation, WMO operational Hydrology Report No. 34, 80 pp

[7] Bentura, P. L. F., and Michel, C. (1997), Flood routing in a wide channel with a quadratic lag-and-route method, Hydrological Sciences-Journal-des Sciences Hydrologiques, 42(2).

[8] Billen, G., Garnier, J., Ficht, A., and Cun, C. (2001), Modeling the response of water quality in the Seine river estuary to human activity in its watershed over the Last 50 Years, Estuarine Research Federation, Vol. 24, No. 6B, p. 977–993.

[9] Bolgov, M. V., Gottschalk, L., Krasovskaia, I., and Moore, R. J. (2002), Hydrological models for environmental management, Kluwer Academic publisher, printed in the Netherlands.

[10] Boroughs, C. B. and Edith A. Z. (2002), Daily Flow Routing with the Muskingum-Cunge Method in the Pecos River RiverWare Model, Proceedings of the Second Federal Interagency Hydrologic Modeling Conference, Las Vegas, NV.

[11] Carter, R. W., and Godfrey, R. G. (1960), Storage and flood routing, US Geological Survey Water Supply Paper, 1543-B:93

[12] Coe, M. T. (1998), A linked global model of terrestrial hydrologic processes: simulation of modern rivers, lakes, and wetlands, Journal of geophysical research, Vol. 103, No. D8, 8885-8899, Apr. 27.

[13] Coe, M. T. (2000), Modeling terrestrial hydrological systems at the continental scale: testing the accuracy of an atmospheric GCM, Journal of Climate, Vol. 13, 686- 704.

[14] Cunge, J. A., (1969), On the subject of a flood propagation computation method (Muskingum Method), J. Hydraulic Res., 7, 205-230.

[15] Dooge, J. C. I. (1973) Linear Theory of Hydrologic Systems. USDA Agricultural Research Service, Tech. Bull. no. 1468, Washington, DC.

[16] Dooge, J. C. I., Strupczewski, W. G., and Napiorkowski, J. J. (1982), Hydrodynamic derivation of storage parameters of the Muskingum model, Journal of Hydrology, 54, 371-387.

[17] Ducharne, A., Baubion, C., Beaudoin, N., Benoit, M., Billen, G., Brisson, N., Garnier, J., Kieken, H., Lebonvallet, S., Ledoux, E., Mary, B., Mignolet, C., Poux, X., Sauboua, E., Schott, C., Théry, S., and Viennot, P. (2007), Long term prospective of the Seine river system: Confronting climatic and direct anthropogenic changes. Science of the Total Environment, 375, 292-311.

[18] Ducharne, A., Koster, R. D., Suarez, M. J., Stieglitz, M., and Kumar, P. (2000), A catchment-based approach to modeling land surface processes in a general circulation model, 2. Parameter estimation and model demonstration, Journal of geophysical research, Vol. 105, No. D20, 24,823-24,838, Oct. 27.

[19] Fette, C.W. (2001), Applied Hydrogeology, Prentice Hall, New Jersey.

[20] Goodwill, I. M., CIVE2400: Fluid Mechanics 2.2, section 2: Open Channel Hydraulics, http://www.efm.leeds.ac.uk/CIVE/CIVE2400/OpenChannelHydraulics2.pdf.

[21] Hannah, D.M., Gurnell A.M. (2001), A conceptual, linear reservoir runoff model to investigate melt season changes in cirque glacier hydrology, Journal of Hydrology, Vol. 246, N° 1, pp. 123-141(19)

[22] Hjelmfelt, A. T. (1985), Negative outflows from Musking flood routing, J. Hdraul. Engng Div., ASCE 111(6), 1010-1014.

[23] Gill, M. A. (1992), Numerical solution of Muskingum equation, J. Hdraul. Engng Div., ASCE 118(5), 804-809.

[24] Kieken, H. (2002), Integrating structural changes in future research and modelling on the Seine River Basin, Integrated Assessment and Decision Support - Proceedings of the 1st Biennial Meeting of the iEMSs, Vol. 2, 37-42.

[25] Koster, R. D., Suarez, M. J., Ducharne, A., Stieglitz, M., and Kumar, P. (2000), A catchment-based approach to modeling land surface processes in a general circulation model, 1. Model structure, Journal of geophysical research, Vol. 105, No. D20, 24,809-24,822, Oct. 27.

[26] Kundzewicz, Z. W., and Strupczewski, W. G. (1982), Approximate translation in the Muskingum model, Hydrological Sciences - Journal - des Sciences Hydrologiques, 27, 1, 19-27.

[27] Lhomme, J., Bouvier, C., and Perrin, J. L. (2004), Applying a GIS-based geomorphological routing model in urban catchments, Journal of Hydrology, 299, 203-216.

[28] Liggett, J. A. (1975), Basic equations of unsteady flow, in Unsteady Flow in Open Channels, Mahmood, K. and Yevjevick, V. (Eds.), Vol. I, Fort Collins, Colorado, Water Resources Publications, pp. 29-62.

[29] Linsley, R. K., M. A. Kohler, and J. L. H. Paulhus (1949), Applied Hydrology, 502-530 pp., Mc Graw Hill Book Co., New York.

[30] Maidment. D. R. (1993), Handbook of Hydrology, McGraw-Hill Professional Publishing, New York.

[31] Masson V., Champeaux J.-L., Chauvin F., Meriguet C., and Lacaze R. (2003). A Global Database of Land Surface Parameters at 1-km Resolution in Meteorological and Climate Models, J. Clim., 16:1261-1282.

[32] McCarthy, G. T. (1939), The unit hydrogroph and flood routing. U.S. Corps Eng., Providence, R.I.

[33] Michel, C., Andréassian, V., Perrin, C., and Bentura, P. (2006), Bi-quadratic store in the lag-and-route method for more efficient flood routing, Water Resources Research, Apr.3.

[34] Napiorkowski, J. J., Strupczewski, W. G., and Dooge, J. C. I. (1981) Lumped nonlinear flood routing model and its simplification to the Muskingum model. In: Proc. Int. Symp. on Rainfall-Runoff Modelling (Mississippi State Univ., May 1981).

[35] Oki, T., Nishimura, T., and Dirmeyer, P. (1999), Assessment of annual runoff from land surface model using total runoff integrating pathways(TRIP), Journal of the Meteorological Society of Japan, Vol. 77, No. 1B, 235-255.

[36] Perumal, M. (1992), The cause of the negative initial outflow with the Muskingum method, Hydrological Sciences-Journal-des Sciences Hydrologiques, 37, 391-401.

[37] Perumal, M. and Sahoo, B. (2007), Applicability criteria of the variable parameter Muskingum stage and discharge routing methods, Water Resources Research, Vol. 43, W05409.

[38] Press, W. H., Teukolsky, S. A., Vetterling, W. T., and Flannery, B. P. (1992), Numerical recipes in Fortran 77- The art scientific computing, Cambridge University Press.

[39] Schulze1, K., Hunger, M., and Döll, P. (2005), Simulating river flow velocity on global scale, Advances in Geosciences, 5, 133–136.

[40] Sherman, L. K. (1932), Stream-flow from rainfall by the unit-graph method, Eng. News-Rec., 108, 501-505.

[41] Sincock, A. M., and M. J. Lees (2002), Extension of the QUASAR river-water quality model to unsteady flow conditions, Journal of the Chartered Institution of Water and Environmental Management, 16, 12-17.

[42] Strupczewski, W, and Kundzewicz, Z. (1980) Muskingum method revisited, J. Hydrol. 48, 327-342.

[43] Tewolde, M. H., and Smithers J. C. (2006), Flood routing in ungauged catchments using Muskingum methods, Water Research Act, Vol. 32, No. 3, 379-388.

[44] Todini, E. (2007), A mass conservative and water storage consistent variable parameter Muskingum-Cunge approach, Hydrology and Earth System Sciences Discussinons, 4, 1549-1592.

[45] Verdin, K. L., and Verdin J. P. (1999), A topological system for delineation and codification of the Earth's river basins, Journal of Hydrology, 218, 1- 12.

[46] Weinmann, P. E., and Laurenson, E. M. (1979), Approximate flood routing methods: A review, J. Hydraulic Div., ASCE, 105 (HY13), Proc., Paper 15057.

[47] Wilson, E. M. (1990), Engineering Hydrology, pp. 110, 196, and 301, Macmillan, Indianapolis, Indiana.

[48] Zbigniew, W. K. (1992), Numerical solution of Muskingum equation, J. Hydraul. Engng Div., ASCE 118(5), 804-809.

Appendixes

Appendix 1. Comparison of the simulated storage according to the numerical method and integration timestep

The figures show the comparisons of the Euler and RK4 results. The storages are simulated after one day, in the different forcing situation described in Tab. 4-1, for different timesteps shown in abscissa.

Case I

Case II

Case III

Case IV
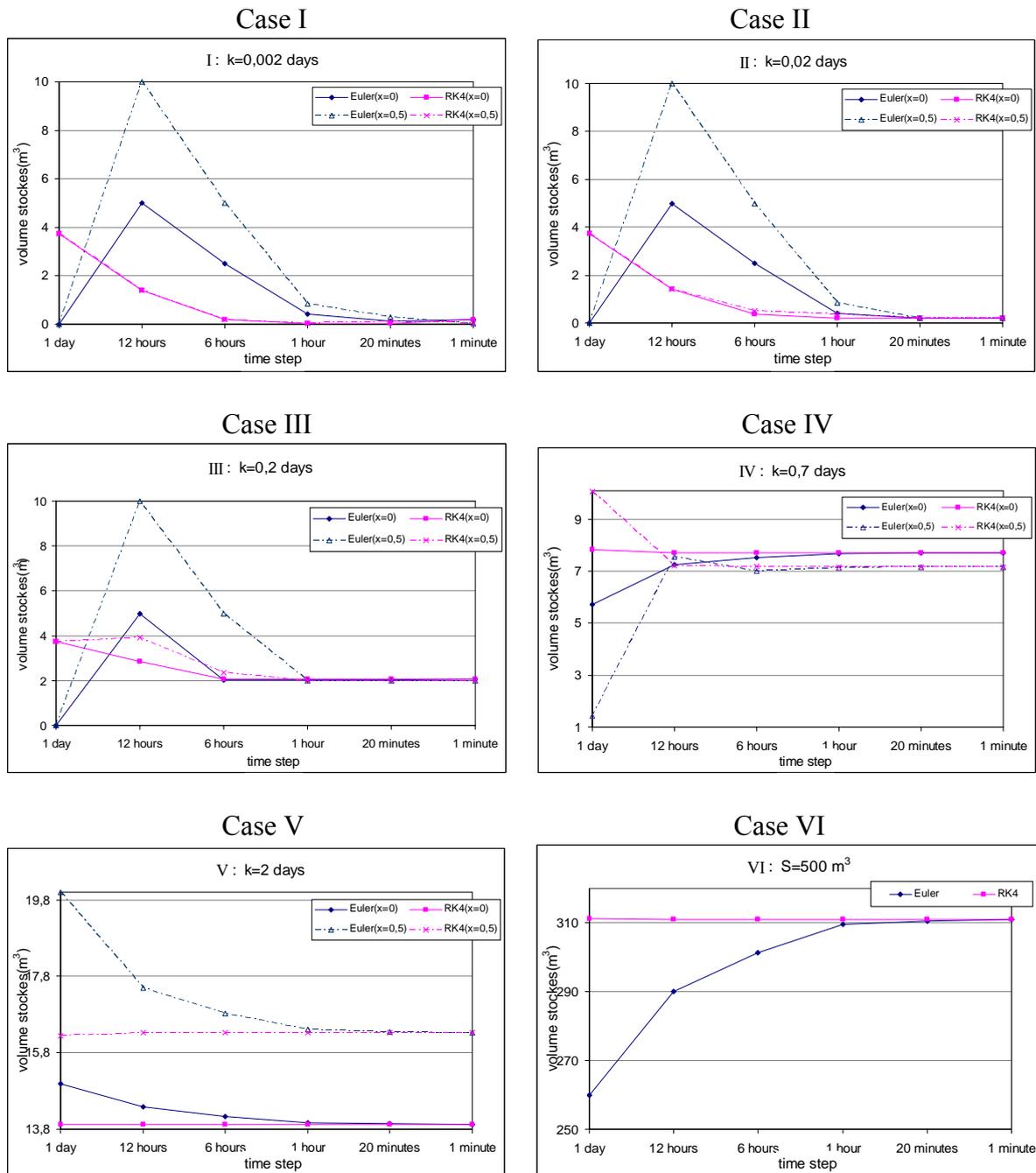
Case V
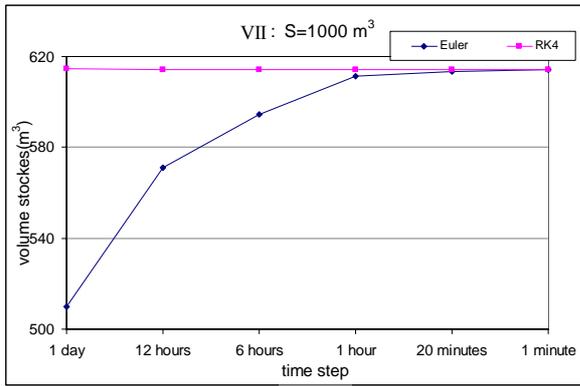
Case VI

Case VII

Case VIII
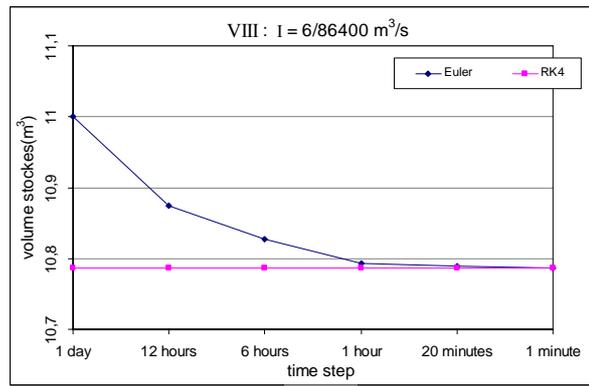
Case IX
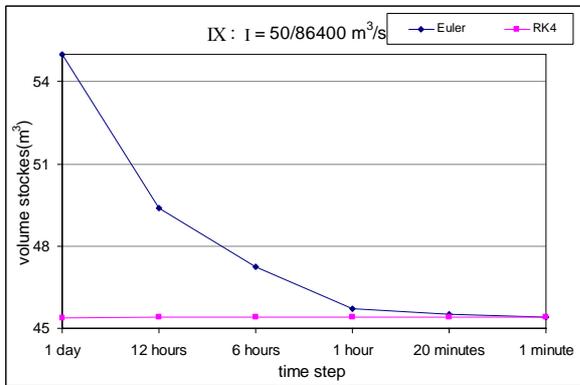
Case X
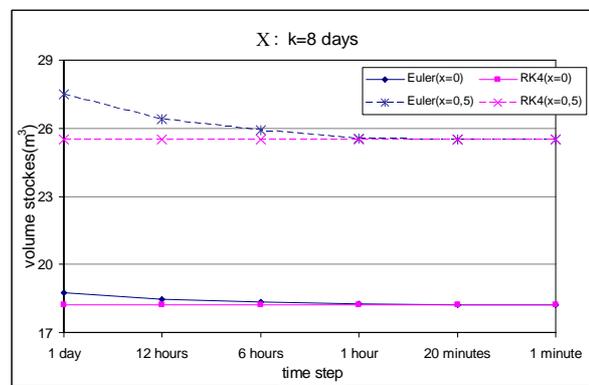
Case XI
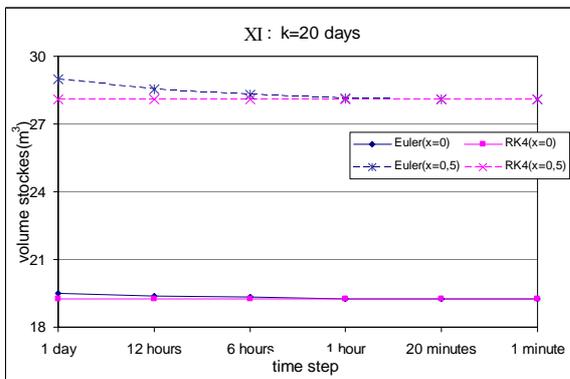
Appendix 2. Comparison of relative error of simulated storage according to the numerical method and integration timestep

Euler with different k (x=0)

I, II, III, IV, V, X, XI : Euler with different k (x = 0)

RK4 with different k (x=0)
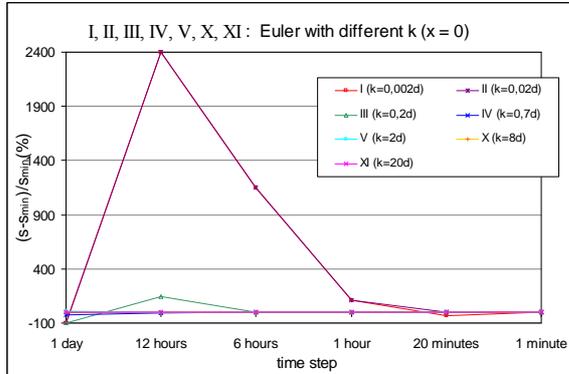
I, II, III, IV, V, X, XI : RK4 with different k (x = 0)

Euler with different k (x=0.5)
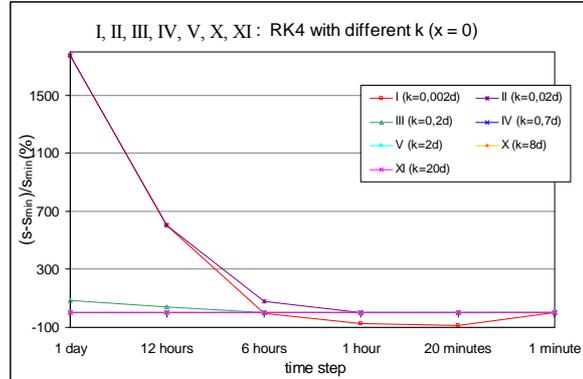
I, II, III, IV, V, X, XI : Euler with different k (x = 0,5)

RK4 with different k (x=0.5)
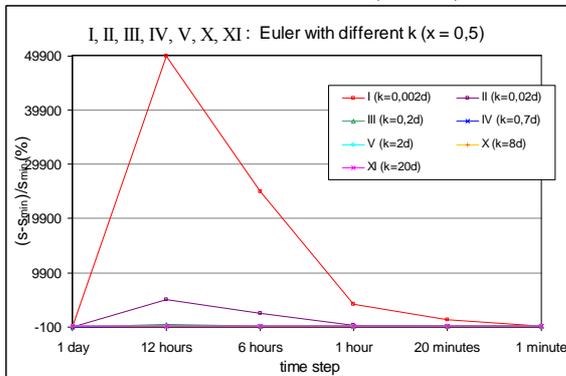
I, II, III, IV, V, X, XI : RK4 with different k (x = 0,5)

Euler with different S
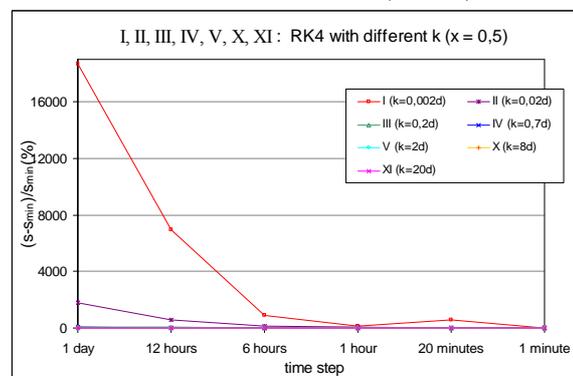
V, VI, VII : Euler with different S

RK4 with different S
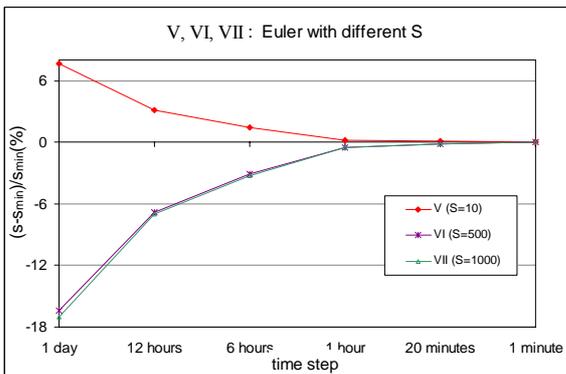
V, VI, VII : RK4 with different S

Euler with different I
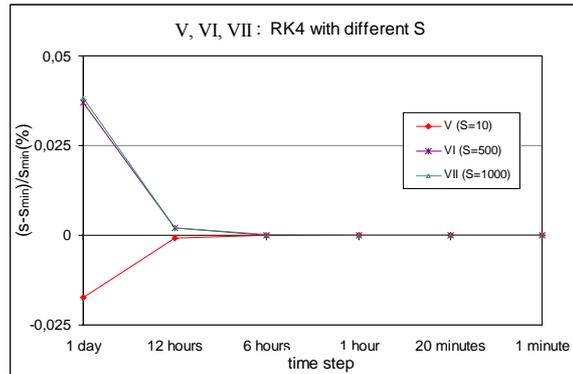
V, VIII, IX : Euler with different I

RK4 with different I
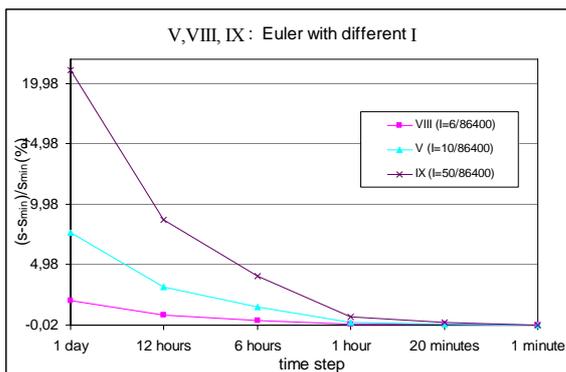
V, VIII, IX : RK4 with different I
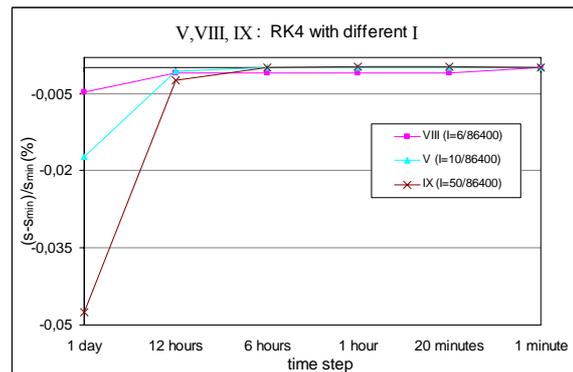
Appendix 3. Figures of sensitivity in a simple reach

3.1 Figures of sensitivity with Muskingum method in a simple reach: The figures in left vertical column are the calculation result with different value of k and x. And those in right column are the results with more values of k when x is fixed to be 0.25.
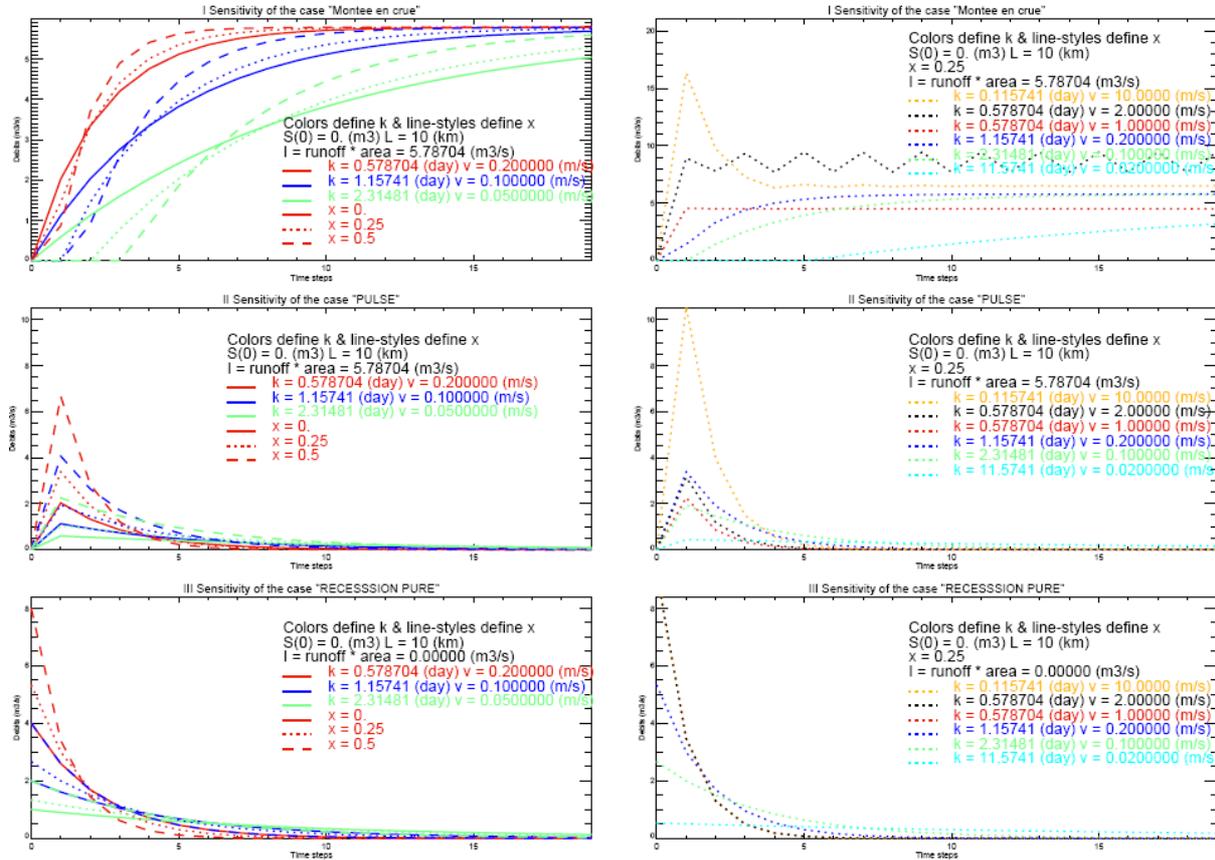
3.2 Figures of sensitivity with Muskingum-and-Manning method in a simple reach: Here are three columns of figures. On the left side, the discharge results with different values of parameters (x, n, s_0, L, T) are presented. In middle there are water depth results, and figures on right side are k computed results with more values of k when x is fixed to be 0.25. Three proposed situations are arranged separately in rows.

III Sensitivity of discharge with different slope in"RECESSSION PURE"   III Sensitivity of water depth with different slope in"RECESSSION PURE"   III Sensitivity of k with different slope in"RECESSSION PURE"

S(0) = 200000. (m3)
L = 10. (km)
T = 3. (m)
x = 0.
n = 0.035
I = runoff * area = 0.00000 (m3/s)
slope = 0.00005
slope = 0.0001
slope = 0.0005
slope = 0.001
slope = 0.005

I Sensitivity of discharge with different length in "Montee en crue"   I Sensitivity of water depth with different length in "Montee en crue"   I Sensitivity of k with different length in "Montee en crue"

S(0) = 0. (m3)
slp = 0.0001 (km)
T = 3. (m)
x = 0.
n = 0.035
I = runoff * area = 5.78704 (m3/s)
L = 1 (km)
L = 25 (km)
L = 50 (km)
L = 75 (km)
L = 100 (km)

II Sensitivity of discharge with different length in "PULSE"   II Sensitivity of water depth with different length in "PULSE"   II Sensitivity of k with different length in "PULSE"

S(0) = 0. (m3)
slp = 0.0001 (km)
T = 3. (m)
x = 0.
n = 0.035
I = runoff * area = 5.78704 (m3/s)
L = 1 (km)
L = 25 (km)
L = 50 (km)
L = 75 (km)
L = 100 (km)

III Sensitivity of discharge with different length in "RECESSSION PURE"   III Sensitivity of water depth with different length in "RECESSSION PURE"   III Sensitivity of k with different length in "RECESSSION PURE"

S(0) = 200000. (m3)
slp = 0.0001 (km)
T = 3. (m)
x = 0.
n = 0.035
I = runoff * area = 0.00000 (m3/s)
L = 1 (km)
L = 25 (km)
L = 50 (km)
L = 75 (km)
L = 100 (km)

I Sensitivity of discharge with different width in "Montee en crue"   I Sensitivity of water depth with different width in "Montee en crue"   I Sensitivity of k with different width in "Montee en crue"

S(0) = 0. (m3)
slp = 0.0001 (km)
L = 10. (km)
x = 0.
n = 0.035
I = runoff * area = 5.78704 (m3/s)
T = 0.5 (m)
T = 1 (m)
T = 5 (m)
T = 25 (m)
T = 50 (m)

II Sensitivity of discharge with different width in "PULSE"   II Sensitivity of water depth with different width in "PULSE"   II Sensitivity of k with different width in "PULSE"

S(0) = 0. (m3)
slp = 0.0001 (km)
L = 10. (km)
x = 0.
n = 0.035
I = runoff * area = 5.78704 (m3/s)
T = 0.5 (m)
T = 1 (m)
T = 5 (m)
T = 25 (m)
T = 50 (m)

III Sensitivity of discharge with different width in"RECESSSION PURE"   III Sensitivity of water depth with different width in"RECESSSION PURE"   III Sensitivity of k with different width in"RECESSSION PURE"

S(0) = 200000. (m3)
slp = 0.0001 (km)
L = 10. (km)
x = 0.
n = 0.035
I = runoff * area = 0.00000 (m3/s)
T = 0.5 (m)
T = 1 (m)
T = 5 (m)
T = 25 (m)
T = 50 (m)

Axis labels: Time steps, Debits (m3/s), Water depth (m), k (day)

Appendix 4. Figures of sensitivity in river network

4.1 Figures of sensitivity with Muskingum method in river network downstream: The figures in left vertical column are the calculation result with different value of k when x is fixed to be 0. And those in right column are the results with the same values of k when x is 0.5.
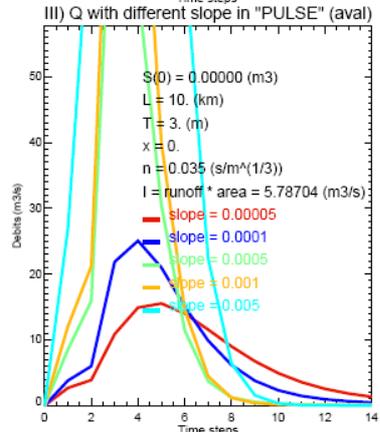
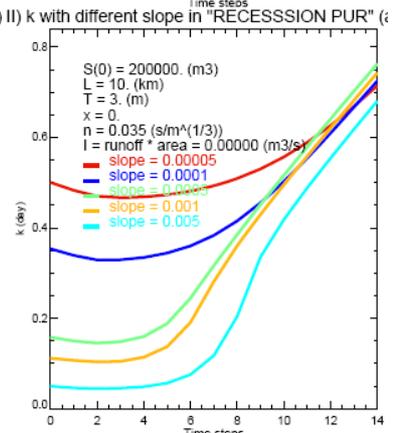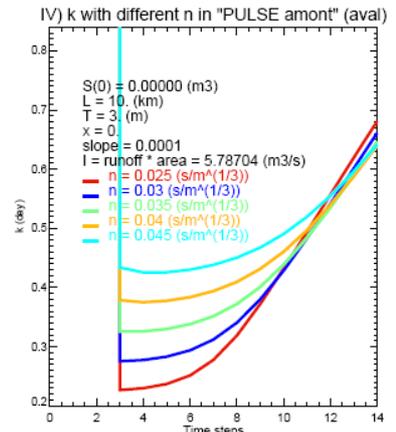III Sensitivity of the case "PULSE amont" (aval)

III Sensitivity of the case "PULSE amont" (aval)

4.2 Figures of sensitivity with Muskingum-and-Manning method in river network downstream: In rows are the simulations in each situation. In columns, from left to right are three results respectively, discharge, water depth and k.
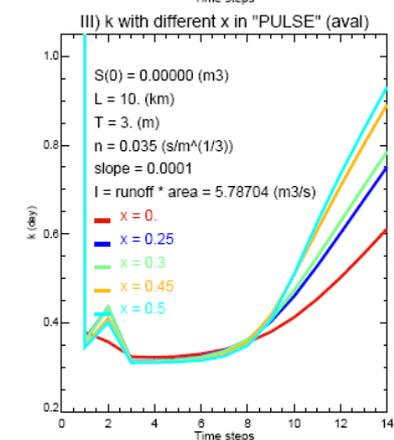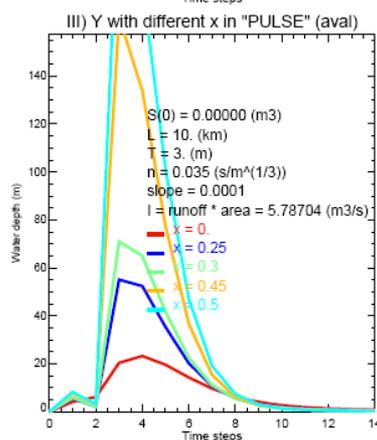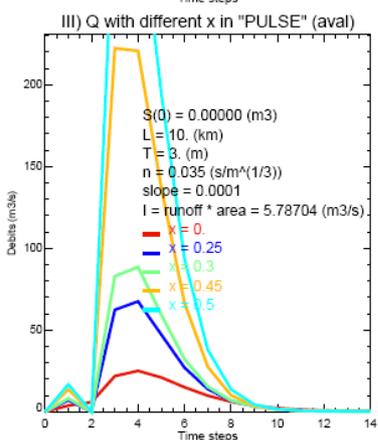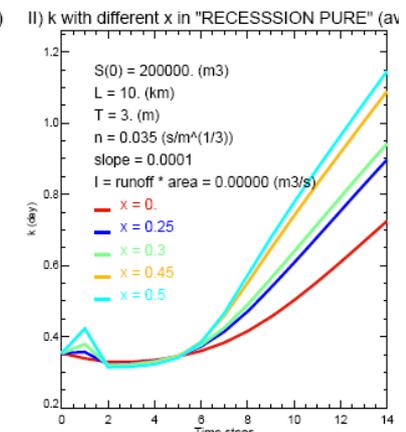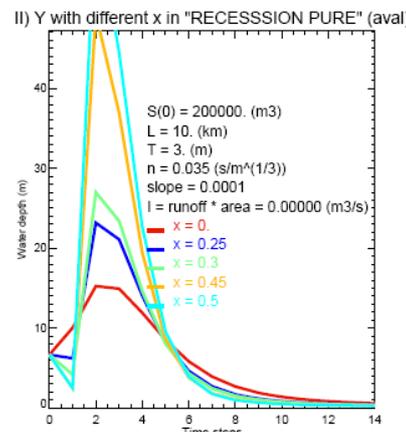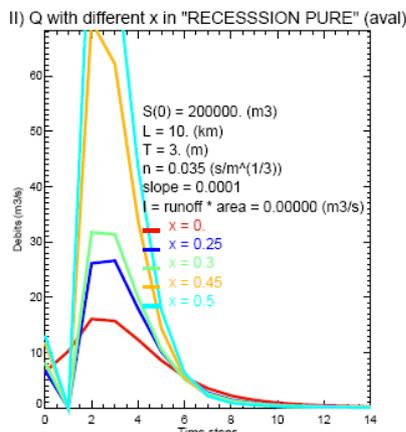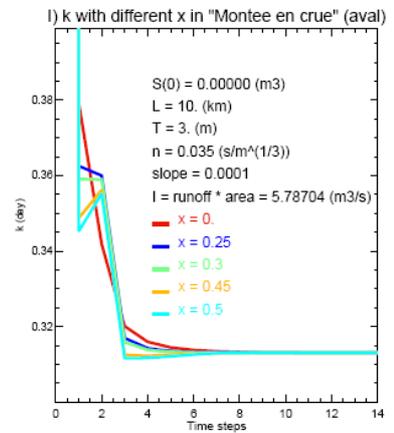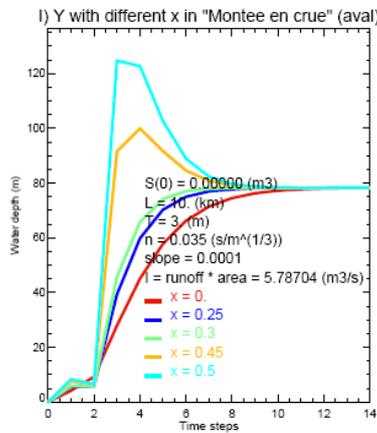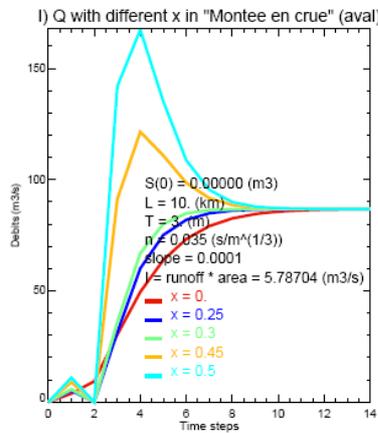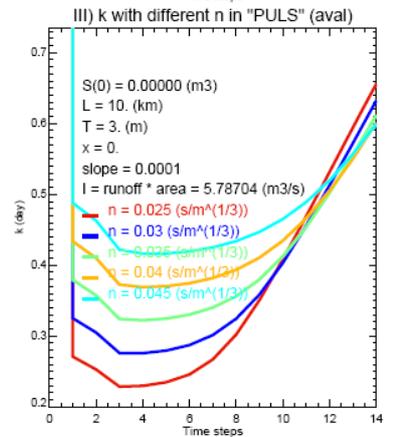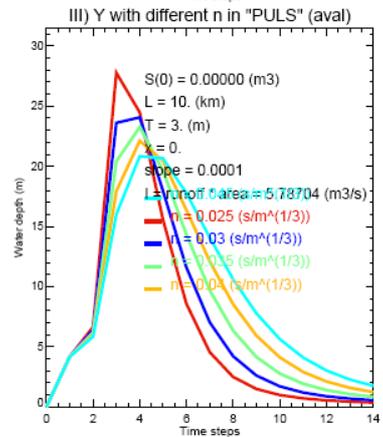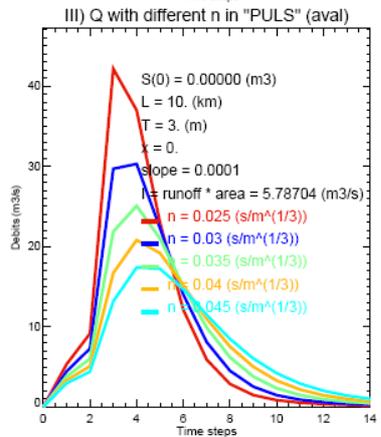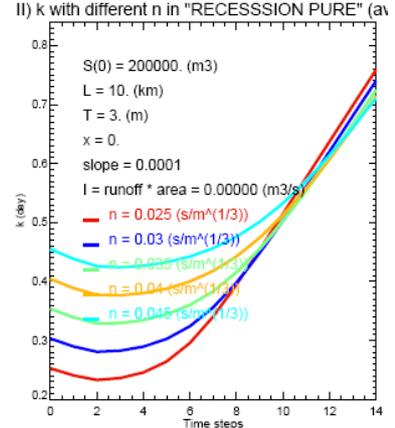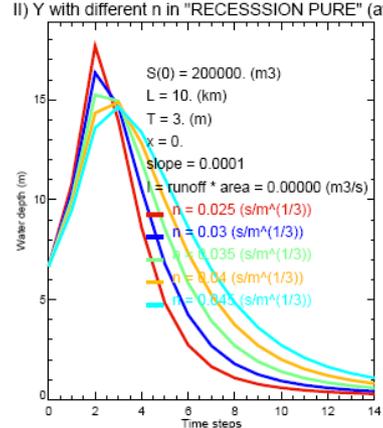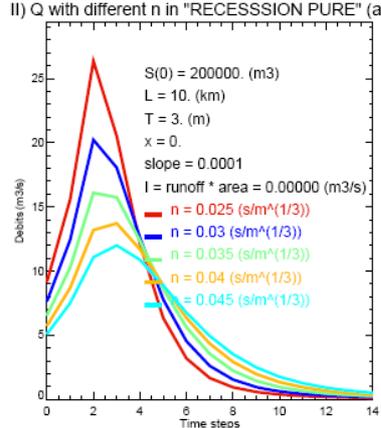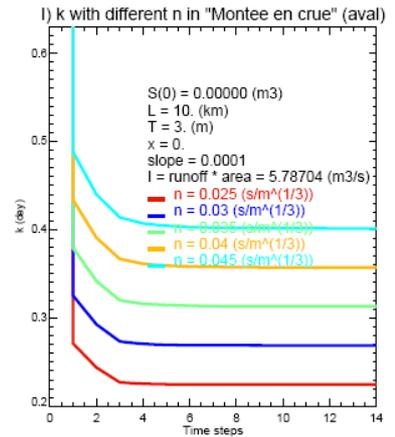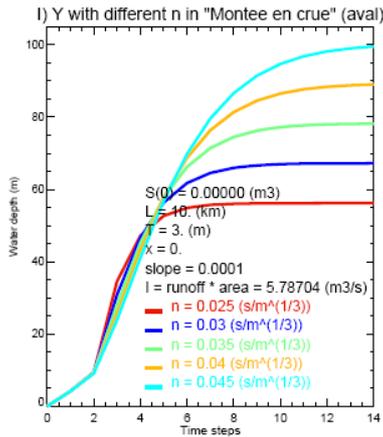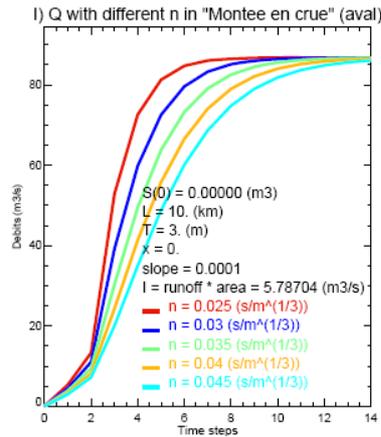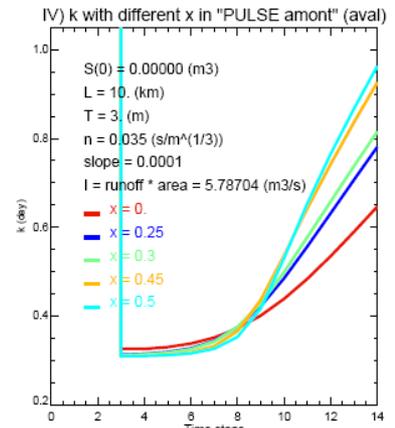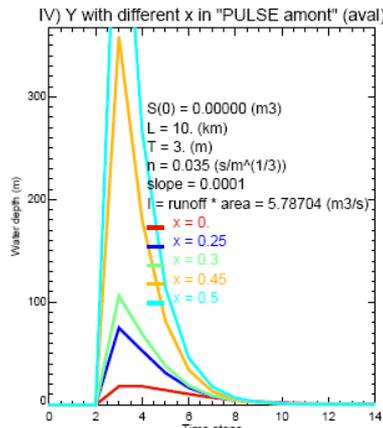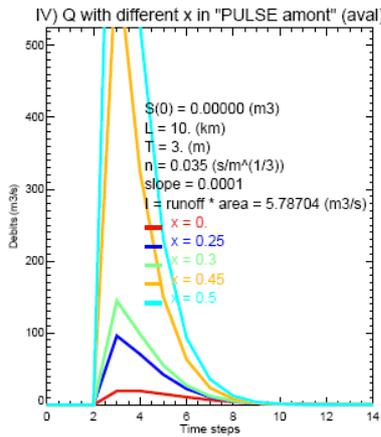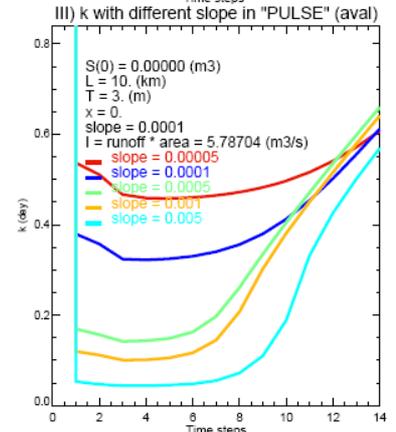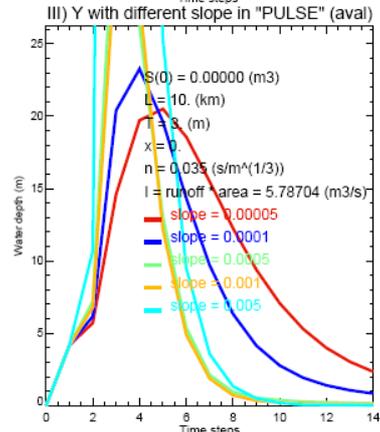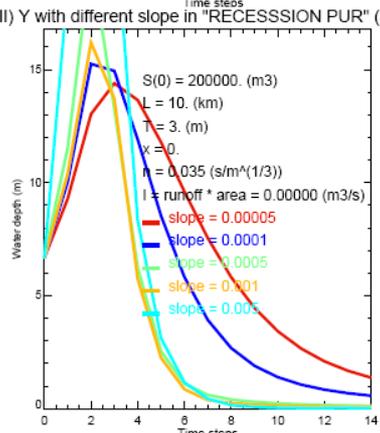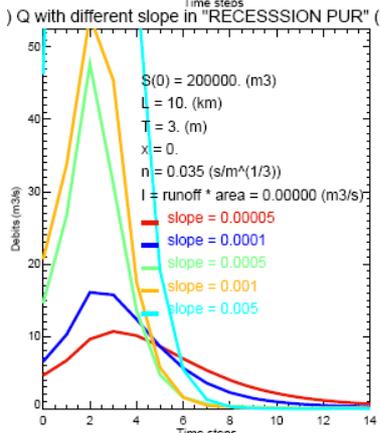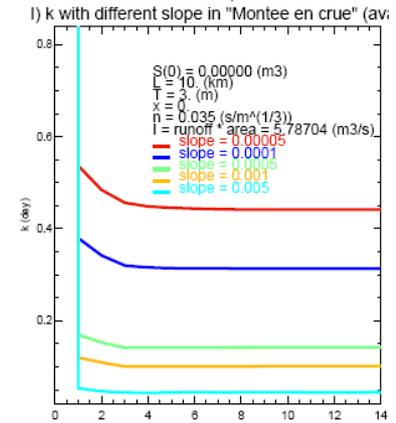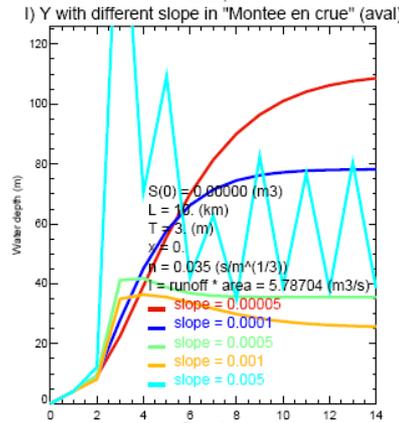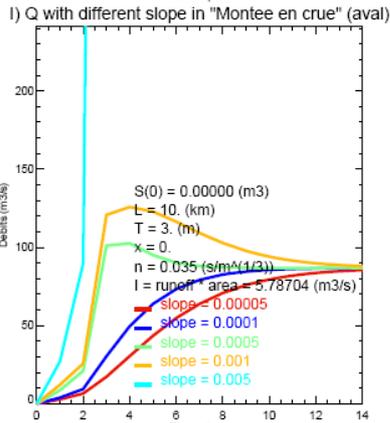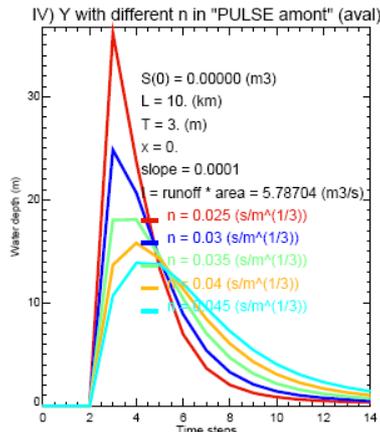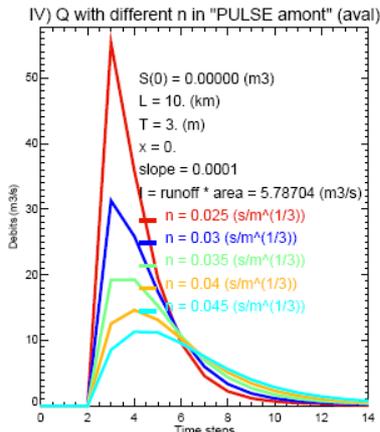
IV) Q with different x in "PULSE amont" (aval)
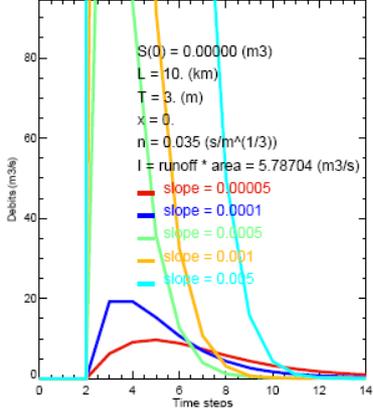
IV) Y with different x in "PULSE amont" (aval)
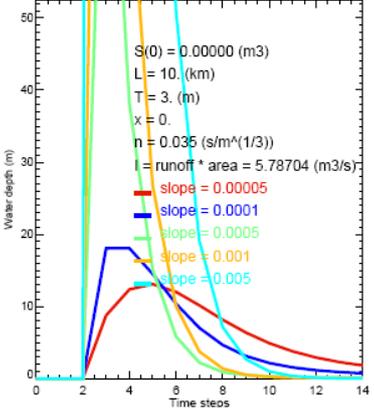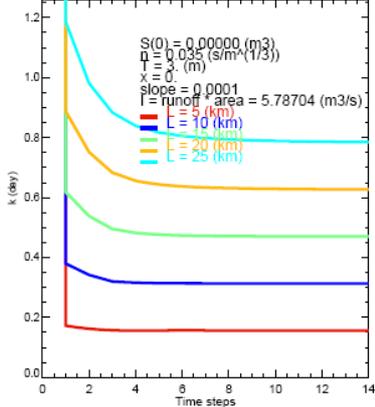
IV) k with different x in "PULSE amont" (aval)
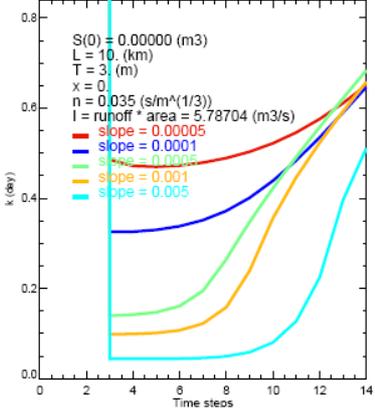
I) Q with different n in "Montee en crue" (aval)
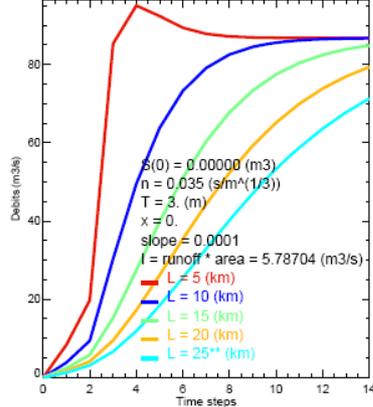
I) Y with different n in "Montee en crue" (aval)
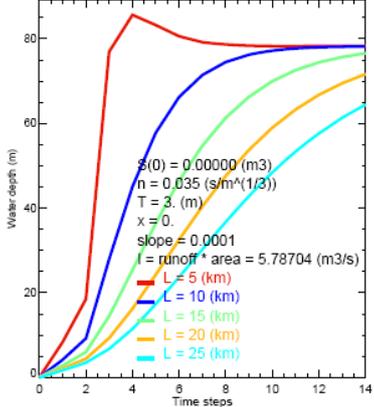
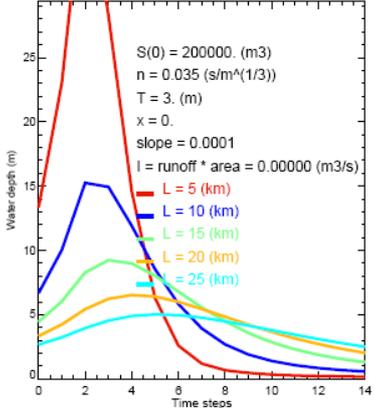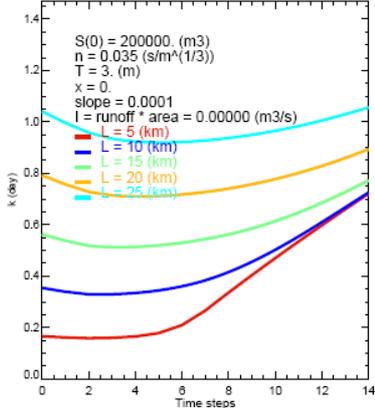I) k with different n in "Montee en crue" (aval)
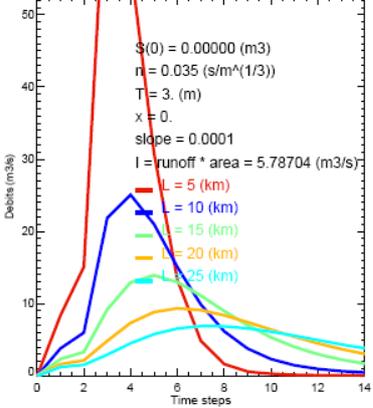
II) Q with different n in "RECESSSION PURE" (aval)
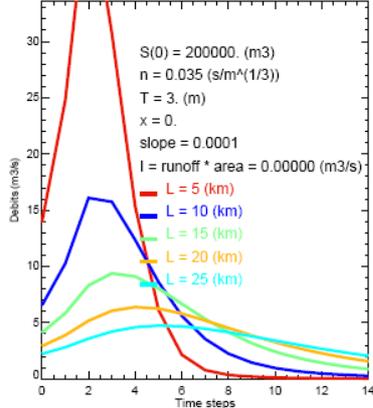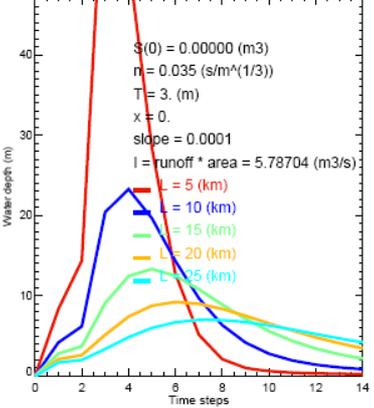
II) Y with different n in "RECESSSION PURE" (aval)
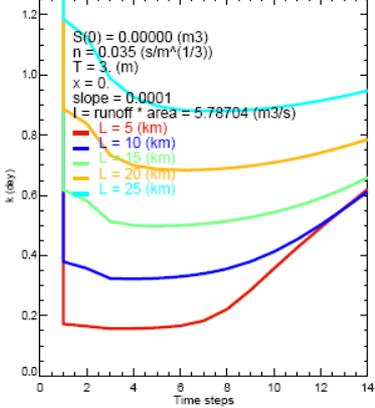
II) k with different n in "RECESSSION PURE" (aval)
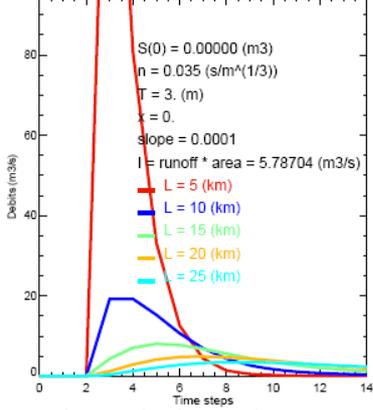
III) Q with different n in "PULS" (aval)

III) Y with different n in "PULS" (aval)

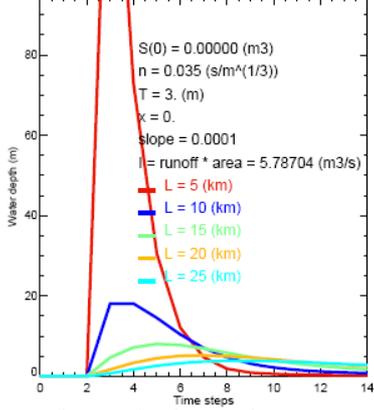III) k with different n in "PULS" (aval)

40

IV) Q with different length in "PULSE amont" (aval)

S(0) = 0.00000 (m3)
n = 0.035 (s/m^(1/3))
T = 3. (m)
x = 0.
slope = 0.0001
I = runoff * area = 5.78704 (m3/s)
L = 5 (km)
L = 10 (km)
L = 15 (km)
L = 20 (km)
L = 25 (km)

IV) Y with different length in "PULSE amont" (aval)

S(0) = 0.00000 (m3)
n = 0.035 (s/m^(1/3))
T = 3. (m)
x = 0.
slope = 0.0001
I = runoff * area = 5.78704 (m3/s)
L = 5 (km)
L = 10 (km)
L = 15 (km)
L = 20 (km)
L = 25 (km)

IV) k with different length in "PULSE amont" (av

S(0) = 0.00000 (m3)
n = 0.035 (s/m^(1/3))
T = 3. (m)
x = 0.
slope = 0.0001
I = runoff * area = 5.78704 (m3/s)
L = 5 (km)
L = 10 (km)
L = 15 (km)
L = 20 (km)
L = 25 (km)

I) Q with different width in "Montee en crue" (aval)

S(0) = 0.00000 (m3)
L = 10. (km)
x = 0.
slope = 0.0001
n = 0.035 (s/m^(1/3))
I = runoff * area = 5.78704 (m3/s)
T = 5 (m)
T = 10 (m)
T = 20 (m)
T = 35 (m)
T = 50 (m)

I) Y with different width in "Montee en crue"" (aval)

S(0) = 0.00000 (m3)
L = 10. (km)
x = 0.
slope = 0.0001
n = 0.035 (s/m^(1/3))
I = runoff * area = 5.78704 (m3/s)
T = 5 (m)
T = 10 (m)
T = 20 (m)
T = 35 (m)
T = 50 (m)

I) k with different width in "Montee en crue" (av

S(0) = 0.00000 (m3)
L = 10. (km)
x = 0.
slope = 0.0001
n = 0.035 (s/m^(1/3))
I = runoff * area = 5.78704 (m3/s)
T = 5 (m)
T = 10 (m)
T = 20 (m)
T = 35 (m)
T = 50 (m)

) Q with different width in "RECESSSION PUR" (aval)

S(0) = 200000. (m3)
L = 10. (km)
x = 0.
slope = 0.0001
n = 0.035 (s/m^(1/3))
I = runoff * area = 0.00000 (m3/s)
T = 5 (m)
T = 10 (m)
T = 20 (m)
T = 35 (m)
T = 50 (m)

II) Y with different width in "RECESSSION PUR" (aval)

S(0) = 200000. (m3)
L = 10. (km)
x = 0.
slope = 0.0001
n = 0.035 (s/m^(1/3))
I = runoff * area = 0.00000 (m3/s)
T = 5 (m)
T = 10 (m)
T = 20 (m)
T = 35 (m)
T = 50 (m)

II) k with different width in "RECESSSION PUR" (a

S(0) = 200000. (m3)
L = 10. (km)
x = 0.
slope = 0.0001
n = 0.035 (s/m^(1/3))
I = runoff * area = 0.00000 (m3/s)
T = 5 (m)
T = 10 (m)
T = 20 (m)
T = 35 (m)
T = 50 (m)

III) Q with different width in "PULSE" (aval)

S(0) = 0.00000 (m3)
L = 10. (km)
x = 0.
slope = 0.0001
n = 0.035 (s/m^(1/3))
I = runoff * area = 5.78704 (m3/s)
T = 5 (m)
T = 10 (m)
T = 20 (m)
T = 35 (m)
T = 50 (m)

III) Y with different width in "PULSE" (aval)

S(0) = 0.00000 (m3)
L = 10. (km)
x = 0.
slope = 0.0001
n = 0.035 (s/m^(1/3))
I = runoff * area = 5.78704 (m3/s)
T = 5 (m)
T = 10 (m)
T = 20 (m)
T = 35 (m)
T = 50 (m)

III) k with different width in "PULSE" (aval)

S(0) = 0.00000 (m3)
L = 10. (km)
x = 0.
slope = 0.0001
n = 0.035 (s/m^(1/3))
I = runoff * area = 5.78704 (m3/s)
T = 5 (m)
T = 10 (m)
T = 20 (m)
T = 35 (m)
T = 50 (m)
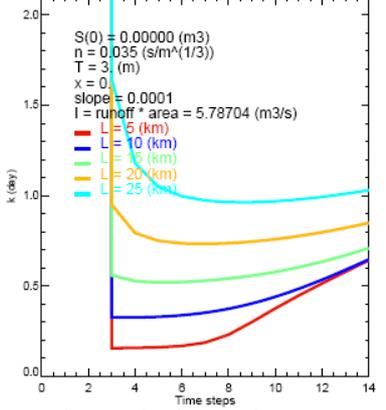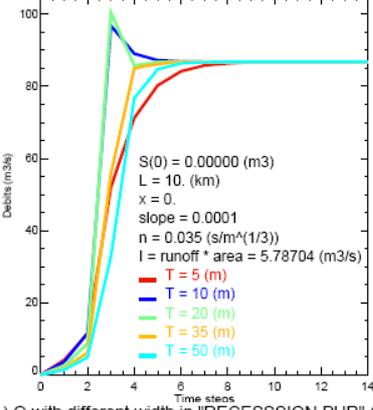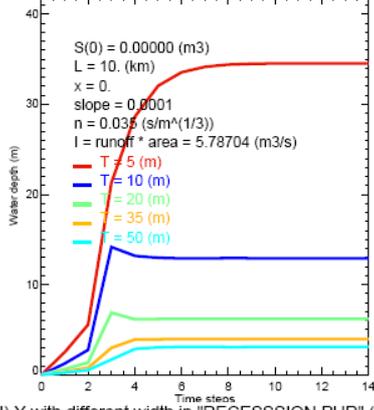
IV) Q with different width in "PULSE amont" (aval)

IV) Y with different width in "PULSE amont" (aval)
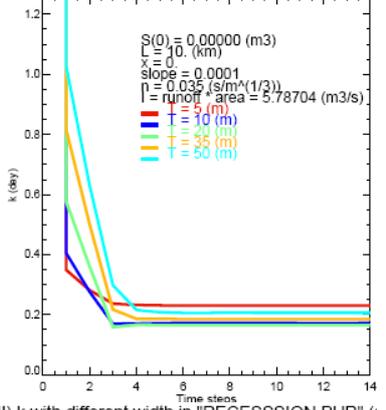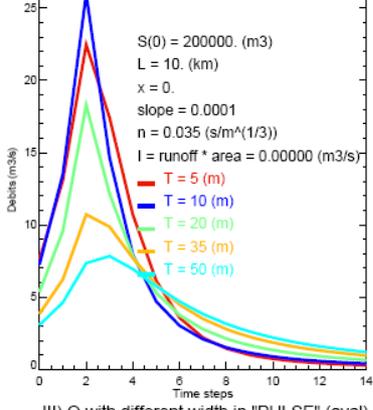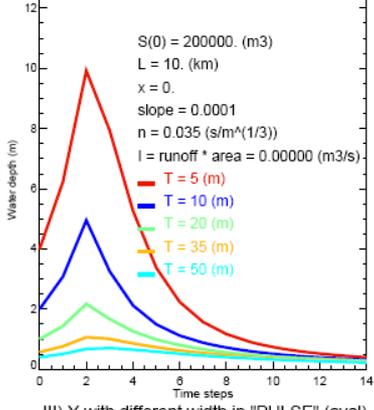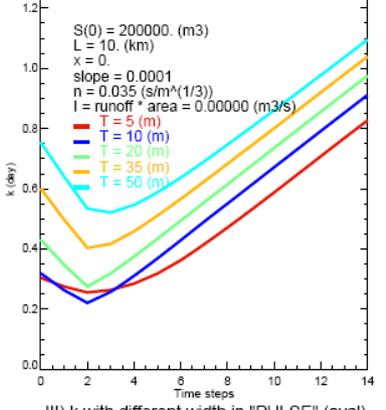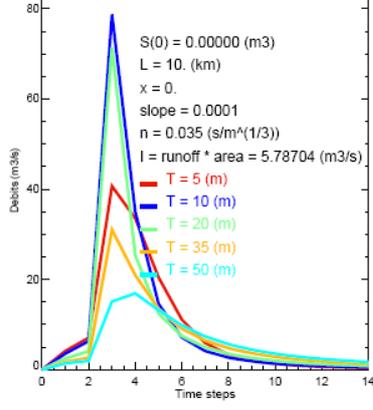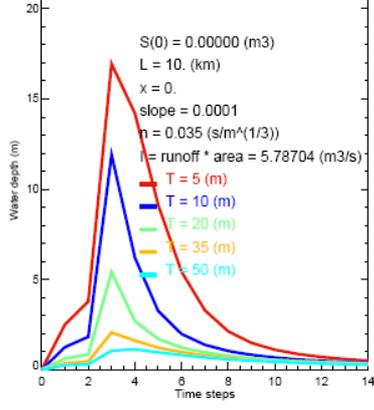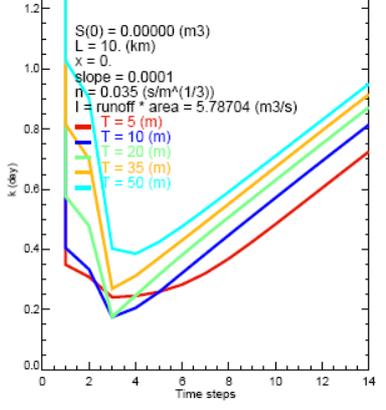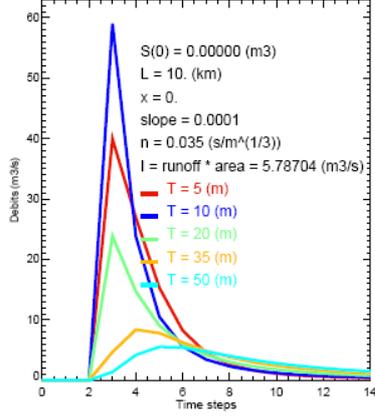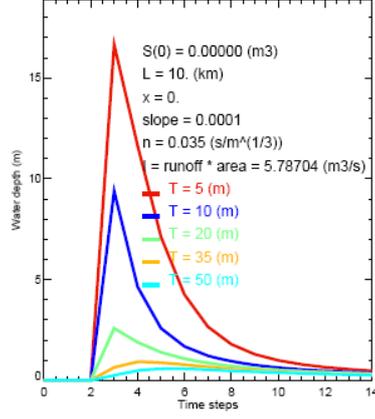
IV) k with different width in "PULSE amont" (av

S(0) = 0.00000 (m3)
L = 10. (km)
x = 0.
slope = 0.0001
n = 0.035 (s/m^(1/3))
I = runoff * area = 5.78704 (m3/s)
T = 5 (m)
T = 10 (m)
T = 20 (m)
T = 35 (m)
T = 50 (m)

44